Journal Pre-proofs

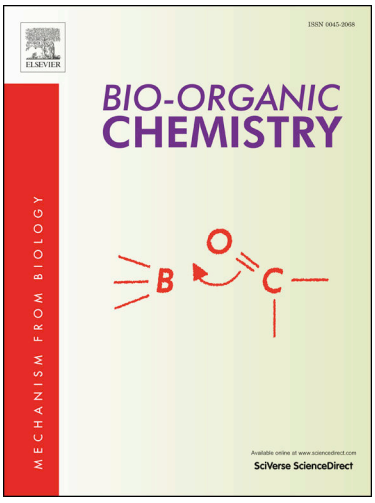

Synthesis and antioxidant activity of conjugates of hydroxytyrosol and coumarin

Wen-Bo Li, Xue-Peng Qiao, Zi-Xiao Wang, Shuai Wang, Shi-Wu Chen

PII: S0045-2068(20)31725-9
DOI: https://doi.org/10.1016/j.bioorg.2020.104427
Reference: YBIOO 104427

To appear in: *Bioorganic Chemistry*

Received Date: 25 September 2020
Revised Date: 20 October 2020
Accepted Date: 21 October 2020

Please cite this article as: W-B. Li, X-P. Qiao, Z-X. Wang, S. Wang, S-W. Chen, Synthesis and antioxidant activity of conjugates of hydroxytyrosol and coumarin, *Bioorganic Chemistry* (2020), doi: https://doi.org/10.1016/j.bioorg.2020.104427

Synthesis and antioxidant activity of conjugates of hydroxytyrosol and coumarin

Wen-Bo Li, Xue-Peng Qiao, Zi-Xiao Wang, Shuai Wang, Shi-Wu Chen *

School of Pharmacy, Lanzhou University, Lanzhou 730000, China

* Corresponding author.

E-mail addresses: chenshw@lzu.edu.cn (S.-W. Chen).

Abstract

Antioxidants have been the subject of intense research interest due to their numerous health benefits. In this work, a series of new conjugates of hydroxytyrosol and coumarin were synthesized and evaluated for their free radical scavenging, toxicity and antioxidant mechanism in vitro. The all target compounds **14a–t** exhibited better radical scavenging activity than BHT, hydroxytyrosol, and coumarin in both DPPH radical and $ABTS^{+}$ radical cation scavenging assays. The structure-activity relationships study indicated that the number and position of hydroxyl groups on the coumarin ring were vital to a good antioxidant capacity. Furthermore, the most promising compound **14q** showed less toxicity in hemolysis assay and weaker antiproliferative effects than BHT against normal WI-38 and GES cells, and enhanced viability of H_2O_2-induced HepG2 cells. Additionally, **14q** decreased the apoptotic percentage of HepG2 cells, reduced the ROS produce and LDH release, and improved GSH and SOD levels in H_2O_2-treated HepG2 cells. Lastly, **14q** exhibited more stability than hydroxytyrosol in methanol solution. These results revealed that conjugations of hydroxytyrosol and coumarin show better antioxidant capacity, and are the efficacious approach to finding novel potential antioxidant.

Keywords: Antioxidant; Free radical scavenging; Conjugates; Coumarin; Hydroxytyrosol

1. Introduction

Oxidation is the most common and ubiquitous chemical reaction that affects both living and non-living forms. Oxygen is vital for the survival of an aerobic organism, however, it leads to the production of free radicals, especially reactive oxygen species (ROS) and reactive nitrogen species (RNS) during biochemical processes. ROS/RNS and initiated chains of biochemical reactions can cause peroxidation of DNA, protein, and lipid, destroy their normal cellular functions, and lead to cell death and apoptosis [1]. To maintain delicate oxidative homeostasis, ROS produced in living cells is continuously neutralized by the antioxidant defense system. Antioxidant defense mechanisms include both enzymatic and non-enzymatic mechanisms. Enzymatic antioxidants comprise of antioxidant enzymes, such as superoxide dismutase (SOD), catalase (CAT), glutathione peroxidase (GSH-Px) and reductase, etc., they are highly specific and detoxify specific free radicals. Non-enzymatic antioxidants, for example, ascorbic acid, Vitamin E, carotenoids, glutathione, etc., are non-specific yet constitute the first line of defense mechanism against free radicals/ROS [2,3].

Antioxidants molecules found in cells are used to prevent free radicals from taking electrons from another molecule. Over the years, significant advancement has been made relating to free radicals and the development of antioxidants. Various kinds of natural, semi-synthetic, as well as synthetic free radical scavengers, have gained much attention as chain-breaking antioxidants that protect aerobic organisms from oxidative damage [4]. Especially, polyphenolic compounds of both natural and synthetic source have drawn greater attention as free radical scavengers [5].

Hydroxytyrosol (**1**, Fig. 1) is the content of *Olives*, also the hydrolysis product and antioxidant active ingredient of glycoside oleuropein (**2**) [6], which possesses many biological activities including anti-oxidation and scavenging free radicals [7], anticancer [8], cardiovascular activity [9], anti-inflammatory [10], antiviral [11], and neural activity [12]. However, the poor stability and deterioration in air or light made it difficult to store [13]. Therefore, it is meaningful to improve its activity and stability by chemical modification, such as esterification [14].

The coumarins are heterocyclic compounds consisting of benzene and 2-pyrone rings enriched in various plants like *tonka beans*. Coumarin and their derivatives exert a vast array of bioactive properties such as antioxidant, anticoagulant, antibacterial, anti-inflammatory, antitumor, antiviral, and enzyme inhibition [15]. Although higher doses of coumarin are found to be hepatotoxic, they exhibit beneficial effects by reducing the risk of cancer and other neuronal and cardiovascular ailments [16]. Most of these effects can be attributed to their free radical scavenging effects. For example, compound **4**, a hybrids of coumarin and chalcone, presents good scavenging capacity, low toxicity, and high cytoprotection [17]. Despite significant advancements in antioxidant searches, coumarins remain one of the most versatile classes of compounds for anti-oxidant drug design and discovery [18].

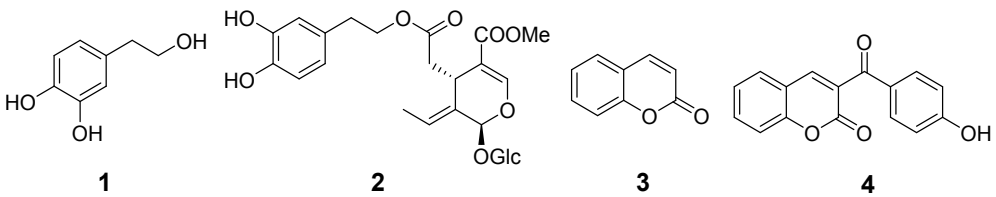

1 **2** **3** **4**

Fig. 1. The chemical structures of hydroxytyrosol (**1**), oleuropein (**2**), coumarin (**3**) and

4.

The conjugation principle involves the rational design of new chemical entities based on the recognition of pharmacophoric subunits with the molecular structure of two or more known bioactive derivatives [19]. The successful fusion of these subunits produces a new conjugate that maintains the desired characteristics of the original subunits. Hence, the conjugation principle in drug discovery is meaningful for the optimization of natural products [20]. As our continuing efforts to find new compounds with potent activities and lower toxicity based on a natural product [21–23], considering the excellent antioxidant activity of the orthodiphenolic moiety and good bio-pharmacological activities of coumarin scaffold, we presented a series of conjugates of coumarin and hydroxytyrosol, in which maintaining the orthodiphenolic moiety of hydroxytyrosol to improve antioxidant activity (Fig. 2). Furthermore, their antioxidative activities and mechanism were also studied.

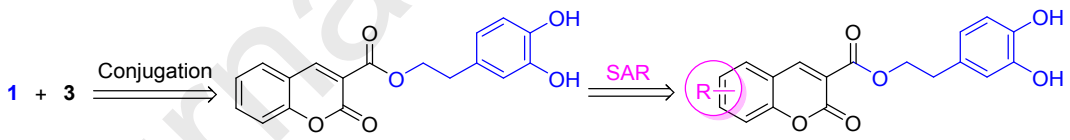

Fig. 2. Design of target compounds.

2. Material and methods

2.1. Reagents and instruments

All materials were obtained from commercial suppliers (Bide Pharmatech Ltd., Shanghai, China and Energy Chemical, Shanghai, China) and were used without further purification, unless stated otherwise. Reaction time was monitored by TLC (silica gel

HRGF254). Column chromatography was performed on silica gel (200–300 mesh) from Yantai Xinnuo Chemicals (Yantai, Shandong, China). All melting points were measured with a Büchi Melting Point X-4 apparatus (Beijing Taike, Beijing, China) and were uncorrected. High-resolution mass spectra (HRMS) were taken in ESI mode on Bruker Apextm Ⅱ 4.7T LC-MS (Bruker, GER). ^{1}H NMR and ^{13}C NMR spectrum were recorded on Agilent-NMR-INOVA600 (Agilent, Palo Alto, CA, USA) with TMS as an internal standard, all chemical shift values were reported as ppm. The purity was measured by HPLC (Waters 1525, US).

2.2. Preparation of the target compounds

2-(3,4-Dihydroxyphenyl)acetic acid **6** as starting material was esterified to give intermediate **7**, which was further protected with benzyl chloride (BnCl), and reduced to yield key intermediate **9** as shown in Scheme 1, with 58% yield for overall 3 steps.

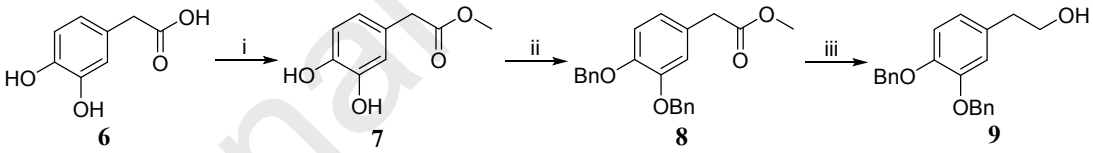

Scheme 1. Reagents and conditions: i) H_2SO_4, MeOH, 75℃; ii) K_2CO_3, BnCl, MeCN, reflux; iii) $LiAlH_4$, THF, 80℃.

The target compounds **14a**–**t** were prepared from *m*-hydroxylbenzaldehydes **10a**–**t** as outlined in Scheme 2. Firstly, ethyl 2-oxo-2*H*-chromene-3-carboxylates (**11a**–**t**) were yielded by Perkin reaction of **10a**–**t** with diethyl carbonate under piperidine catalysis. Then **11a**–**t** were changed into **12a**–**t** by hydrolysis directly in the presence of 10% NaOH, or after benzyl protection of hydroxyl group with benzyl chloride

(BnCl). And carboxylic acids **12a**–**t** were esterified with **9** using 1-(3-dimethylaminopropyl)-3-ethylcarbodiimide hydrochloride (EDC·HCl) and *N,N*-dimethylaminopyridine (DMAP) catalysis to give **13a**–**t**. Finally, the targets **14a**–**t** were obtained by deprotection of **13a**–**t** with BBr_3.

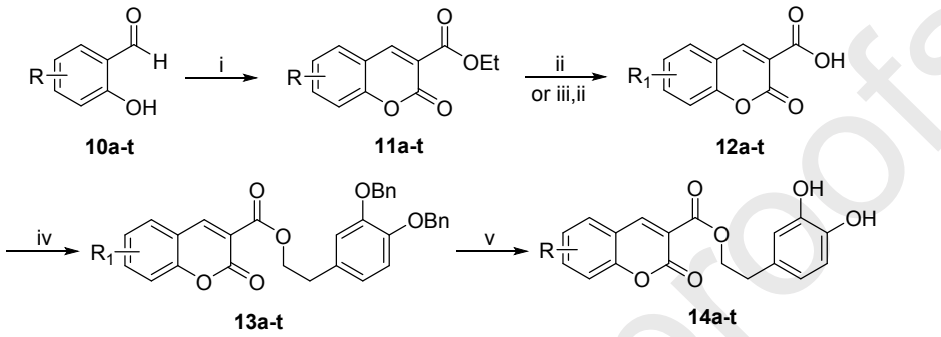

a R=R$_1$= H **b** R=R$_1$= 6-CH$_3$ **c** R=R$_1$= 6-Cl **d** R= 6-OH, R$_1$= 6-OBn
e R=R$_1$= 6-OCH$_3$ **f** R=R$_1$= 6-NO$_2$ **g** R=R$_1$= 7-CH$_3$ **h** R=R$_1$= 7-Cl
i R= 7-OH, R$_1$= 7-OBn **j** R=R$_1$= 7-OCH$_3$ **k** R=R$_1$= 8-CH$_3$ **l** R=R$_1$= 8-Cl
m R= 8-OH, R$_1$= 8-OBn **n** R=R$_1$= 8-OCH$_3$ **o** R=R$_1$= 5,7-OCH$_3$ **p** R=R$_1$= 6,8-C(CH$_3$)$_3$
q R= 7,8-OH, R$_1$= 7,8-OBn **r** R=R$_1$= 7,8-OCH$_3$ **s** R=R$_1$= 6,8-Cl **t** R=R$_1$= 5,6-phenyl ring

Scheme 2. Reagents and conditions: i) diethyl carbonate, piperidine, CH_3COOH, 75℃; ii) 10% NaOH, EtOH, heat; iii) Cs_2CO_3, BnCl, DMF, 80℃; iv) **9**, EDCI, DMAP, CH_2Cl_2, rt; v) BBr_3 (1 M in CH_2Cl_2), CH_2Cl_2, –40℃.

2.2.1. Synthetic procedure of compound 7

To a solution of 3,4-dihydroxyphenylacetic acid **6** (5.65 g, 33.6 mmol) in MeOH (100 mL), H_2SO_4 (98%, 10 drops) was slowly added in atmosphere of argon, followed by further refluxing for 6 h. After the reaction was completed, the solution was concentrated under reduced pressure. The residue was dissolved in ethyl acetate (30 mL), and the solution was washed with saturated $NaHCO_3$ solution. The aqueous phase was extracted with ethyl acetate (20 mL×3), washed with saturated NaCl solution (20 mL), dried over anhydrous Na_2SO_4, and evaporated in vacuo to give the crude product **7**, which was directly used in the next step without further purification.

*2.2.2. Synthetic procedure of compound **8***

A solution of benzyl chloride (BnCl, 11.5 mL, 100 mmol), potassium carbonate (K_2CO_3, 13.8 g, 100 mmol) and **7** in MeCN (80 mL) was stirred for 24 h at 80 ℃ in atmosphere of argon. Next, the solvent was evaporated under vacuum, and the residue was dissolved in ethyl acetate (30 mL) and washed with H_2O (20 mL). Then aqueous phase was extracted with ethyl acetate (20 ml×3), washed with saturated NaCl (20 ml), dried over Na_2SO_4, and filtered. The solvent was evaporated in vacuo, and purified by column chromatography (PE: EA = 20:1) to give **8** as a colorless liquid. Yield: 64% (two steps); ^{1}H NMR (600 MHz, $CDCl_3$): δ 7.46–7.25 (m, 10H), 6.90–6.77 (m, 3H), 5.15 (s, 2H), 5.14 (s, 2H), 3.65 (s, 3H), 3.51 (s, 2H).

*2.2.3. Synthetic procedure of compound **9***

To a solution of **8** (11.3 g, 31.2 mmol) in dry THF (80 mL), lithium tetrahydroaluminum ($LiAlH_4$, 0.59 g, 15.6 mmol) was slowly added in atmosphere of argon. The mixture was warmed to 80℃ and stirred for 4 h. Then, the resulting mixture was cooled to room temperature, and water/ether (1:1) was added to quench the reaction. The organic extracts were filtered, and evaporated in vacuo. The crude product was purified by column chromatography (PE: EA = 5:1) to provide 2-(3,4-Bis(benzyloxy)phenyl)ethan-1-ol (**9**) (9.48 g, 28.4 mmol) as white solid; Yield: 91%; ^{1}H NMR (600 MHz, $CDCl_3$): δ 7.46–7.25 (m, 10H), 6.90–6.77 (m, 3H), 5.15 (s, 2H), 5.14 (s, 2H), 3.65 (s, 3H), 3.51 (s, 2H).

*2.2.4. General synthetic procedure of compounds **11a–t***

Compounds **10** (10 mmol) and diethyl malonate (20 mmol) in EtOH (20 mL) were added piperidine (2.5 mmol) and AcOH (2 drops). Following the reaction mixture was warmed to 75℃ and stirred for 1 h. The mixture was poured into the cold water to yield a large amount of solid. The solid product was filtered off and recrystallized with H_2O/EtOH to afford compounds **11a–t** in good yields, while **11g**, **11j**, and **11p** were used directly in the next reaction without purification.

*2.2.4.1. Ethyl 2-oxo-2H-chromene-3-carboxylate (**11a**)*. Yield: 82%; white solid; ^{1}H NMR (600 MHz, DMSO-d_6): δ 8.74 (s, 1H), 7.92–7.39 (m, 3H), 4.29 (q, 2H, J = 7.2 Hz), 1.30 (t, 3H, J = 7.2 Hz).

*2.2.4.2. Ethyl 6-methyl-2-oxo-2H-chromene-3-carboxylate (**11b**)*. Yield: 88%; yellow solid; ^{1}H NMR (600 MHz, DMSO-d_6): δ 8.68 (s, 1H), 7.70–7.34 (m, 3H), 4.30 (q, 2H, J = 7.2Hz), 2.38 (s, 3H), 1.31 (t, 3H, J = 7.2 Hz).

*2.2.4.3. Ethyl 6-chloro-2-oxo-2H-chromene-3-carboxylate (**11c**)*. Yield: 92%; white solid; ^{1}H NMR (600 MHz, DMSO-d_6): δ 8.72 (s, 1H), 8.06–7.48 (m, 3H), 4.31 (q, 2H, J = *7.2* Hz), 1.32 (t, 3H, J = 7.2 Hz).

*2.2.4.4. Ethyl 6-hydroxy-2-oxo-2H-chromene-3-carboxylate (**11d**)*. Yield: 86%; yellow solid; ^{1}H NMR (600 MHz, DMSO-d_6): δ 9.91 (s, 1H), 8.67 (s, 1H), 7.30–7.15 (m, 3H), 4.29 (q, 2H, J = 6.6 Hz), 1.31 (t, 3H, J = 6.6 Hz).

*2.2.4.5. Ethyl 6-methoxy-2-oxo-2H-chromene-3-carboxylate (**11e**)*. Yield: 83%; red solid; ^{1}H NMR (600 MHz, DMSO-d_6) δ 8.71 (s, 1H), 7.50–7.33 (m, 3H), 4.30 (q, 2H, J = 6.6 Hz), 3.82 (s, 3H), 1.31 (t, 3H, J = 6.6 Hz).

*4.1.4.6. Ethyl 6-nitro-2-oxo-2H-chromene-3-carboxylate (**11f**)*. Yield: 86%; brown

solid; ^{1}H NMR (600 MHz, DMSO-d_6): δ 8.94 (s, 1H), 8.93–87.66 (m, 3H), 4.33 (q, 2H, J = 6.6 Hz), 1.33 (t, 3H, J = 6.6 Hz).

*2.2.4.7. Ethyl 7-chloro-2-oxo-2H-chromene-3-carboxylate (**11h**)*. Yield: 67%; yellow solid; ^{1}H NMR (600 MHz, DMSO-d_6): δ 8.78 (s, 1H), 7.96–7.49 (m, 3H), 4.30 (q, 2H, J = 7.2 Hz), 1.31 (t, 3H, J = 7.2 Hz).

*2.2.4.8. Ethyl 7-hydroxy-2-oxo-2H-chromene-3-carboxylate (**11i**)*. Yield: 75%; white solid; ^{1}H NMR (600 MHz, DMSO-d_6): δ 10.68 (s, 1H), 8.53 (s, 1H), 7.53–6.77 (m, 3H), 4.35 (q, 2H, J = 7.2 Hz), 1.39 (t, 3H, J = 7.2 Hz).

*2.2.4.9. Ethyl 8-methyl-2-oxo-2H-chromene-3-carboxylate (**11k**)*. Yield: 82%; white solid; ^{1}H NMR (600 MHz, DMSO-d_6): δ 8.73 (s, 1H), 7.75–7.30 (m, 3H), 4.30 (q, 2H, J = 6.6 Hz), 2.37 (s, 3H), 1.32 (t, 3H, J = 6.6 Hz).

*2.2.4.10. Ethyl 8-chloro-2-oxo-2H-chromene-3-carboxylate (**11l**)*. Yield: 62%; yellow solid; ^{1}H NMR (600 MHz, DMSO-d_6): δ 8.80 (s, 1H), 7.92–7.41 (m, 3H), 4.31 (q, 2H, J = 7.2 Hz), 1.32 (t, 3H, J = 7.2 Hz).

*2.2.4.11. Ethyl 8-hydroxy-2-oxo-2H-chromene-3-carboxylate (**11m**)*. Yield: 90%; white solid; ^{1}H NMR (600 MHz, DMSO-d_6): δ 10.39 (s, 1H), 8.68 (s, 1H), 7.32–7.19 (m, 3H), 4.27 (q, 2H, J = 7.2 Hz), 1.29 (t, 3H, J = 7.2 Hz).

*2.2.4.12. Ethyl 8-methoxy-2-oxo-2H-chromene-3-carboxylate (**11n**)*. Yield: 78%; red solid; ^{1}H NMR (600 MHz, DMSO-d_6): δ 8.72 (s, 1H), 7.45–7.32 (m, 3H), 4.28 (q, 2H, J = 6.6 Hz), 3.90 (s, 3H), 1.29 (t, 3H, J = 6.6 Hz).

*2.2.4.13. Ethyl 5,7-dimethoxy-2-oxo-2H-chromene-3-carboxylate (**11o**)*. Yield: 87%; green solid; ^{1}H NMR (600 MHz, DMSO-d_6): δ 8.61 (s, 1H), 6.64–6.55 (m, 2H), 4.26

(q, 2H, *J* = 6.6 Hz), 3.95 (s, 3H), 3.90 (s, 3H), 1.29 (t, 3H, *J* = 6.6 Hz).

*2.2.4.14. Ethyl 7,8-dihydroxy-2-oxo-2H-chromene-3-carboxylate (**11q**)*. Yield: 80%; green solid; ^{1}H NMR (600 MHz, DMSO-d_6): δ 8.62 (s, 1H), 7.26–6.84 (m, 2H), 4.24 (q, 2H, *J* = 7.2 Hz), 1.28 (t, 3H, *J* = 7.2 Hz).

*2.2.4.15. Ethyl 7,8-dimethoxy-2-oxo-2H-chromene-3-carboxylate (**11r**)*. Yield: 97%; white solid; ^{1}H NMR (600 MHz, DMSO-d_6): δ 8.71 (s, 1H), 7.68–7.18 (m, 2H), 4.27 (q, 2H, *J* = 7.2 Hz), 3.95 (s, 3H), 3.83 (s, 3H), 1.30 (t, 3H, *J* =7.2 Hz).

*2.2.4.16. Ethyl 6,8-dichloro-2-oxo-2H-chromene-3-carboxylate (**11s**)*. Yield: 93%; white solid; ^{1}H NMR (600 MHz, DMSO-d_6): δ 8.73 (s, 1H), 8.08–8.05 (m, 2H), 4.32 (q, 2H, *J* = 7.2 Hz), 1.32 (t, 3H, *J* = 7.2 Hz).

*2.2.4.17. Ethyl 3-oxo-3H-benzo[f]chromene-2-carboxylate (**11t**)*. Yield: 89%; yellow solid; ^{1}H NMR (600 MHz, DMSO-d_6): δ 9.34 (s, 1H), 8.57–8.06 (m, 3H), 7.79–7.57 (m, 3H), 4.35 (q, 2H, *J* = 7.2 Hz), 1.37 (t, 3H, *J* = 7.2 Hz).

*2.2.5. General synthetic procedure of compounds **12a–t***

Compound **11** (5 mmol) in EtOH (5 mL) were added 10% NaOH (10 mL). Next, the mixture was warmed to 80℃ and stirred for 15 min. The resulting mixture poured off in cold water to precipitate a large amount of solid product. The solid product was filtered off and recrystallized by EtOH to afford acid compounds **12a–t** (except **12d**, **12i**, **12m**, and **12q**) in good yields.

For compounds **12d**, **12i, 12m**, and **12q**, compounds **11d**, **11i**, **11m**, and **11q** (2.46 mmol) were firstly protected with BnCl (7.37 mmol) in the presence of K_2CO_3 (7.37 mmol) in DMF (15mL). Then a similar procedure of **11a** was performed to provide

desired compounds **12d**, **12i, 12m**, and **12q**.

*2.2.5.1. 2-Oxo-2H-chromene-3-carboxylic acid (**12a**)*. Yield: 82%; white solid; ^{1}H NMR (600 MHz, DMSO-d_6): δ 8.74 (s, 1H), 7.91–7.39 (m, 3H).

*2.2.5.2. 6-Methyl-2-oxo-2H-chromene-3-carboxylic acid (**12b**)*. Yield: 92%; green solid; ^{1}H NMR (600 MHz, DMSO-d_6): δ 8.70 (s, 1H), 8.04–7.48 (m, 3H), 2.51 (s, 3H).

*2.2.5.3. 6-Chloro-2-oxo-2H-chromene-3-carboxylic acid (**12c**)*. Yield: 86%; yellow solid; ^{1}H NMR (600 MHz, DMSO-d_6): δ 8.66 (s, 1H), 7.68–7.33 (m, 3H), 2.38 (s, 3H).

*2.2.5.4. 6-(Benzyloxy)-2-oxo-2H-chromene-3-carboxylic acid (**12d**)*. Yield: 94%; yellow solid; ^{1}H NMR (600 MHz, DMSO-d_6): δ 8.69 (s, 1H), 7.57–7.34 (m, 8H), 5.16 (s, 1H).

*2.2.5.5. 6-Methoxy-2-oxo-2H-chromene-3-carboxylic acid (**12e**)*. Yield: 82%; yellow solid; ^{1}H NMR (600 MHz, DMSO-d_6): δ 8.70 (s, 1H), 7.48–7.32 (m, 3H), 3.82 (s, 3H).

*2.2.5.6. 6-Nitro-2-oxo-2H-chromene-3-carboxylic acid (**12f**)*. Yield: 84%; yellow solid; ^{1}H NMR (600 MHz, DMSO-d_6): δ 8.91-8.89 (m, 2H), 7.64–8.50 (m, 2H).

*2.2.5.7. 7-Methyl-2-oxo-2H-chromene-3-carboxylic acid (**12g**)*. Yield: 91%; white solid; ^{1}H NMR (600 MHz, DMSO-d_6): δ 8.72 (s, 1H), 7.79–7.24 (m, 3H).

*2.2.5.8. 7-Chloro-2-oxo-2H-chromene-3-carboxylic acid (**12h**)*. Yield: 86%; white solid; ^{1}H NMR (600 MHz, DMSO-d_6): δ 8.65 (s, 1H), 7.92–7.46 (m, 3H).

*2.2.5.9. 7-(Benzyloxy)-2-oxo-2H-chromene-3-carboxylic acid (**12i**)*. Yield: 95%; yellow solid; ^{1}H NMR (600 MHz, DMSO-d_6): δ 8.70 (s, 1H), 7.83–7.05 (m, 8H), 5.24 (s, 2H).

*2.2.5.10. 7-Methoxy-2-oxo-2H-chromene-3-carboxylic acid (**12j**)*. Yield: 90%; red

solid; ^{1}H NMR (600 MHz, DMSO-d_6): δ 8.71 (s, 1H), 7.83–6.99 (m, 3H), 3.89(s, 3H).

*2.2.5.11. 8-Methyl-2-oxo-2H-chromene-3-carboxylic acid (**12k**)*. Yield: 72%; white solid; ^{1}H NMR (600 MHz, DMSO-d_6): δ 8.73 (s, 1H), 7.74–7.29 (m, 3H), 2.37 (s, 3H).

*2.2.5.12. 8-Chloro-2-oxo-2H-chromene-3-carboxylic acid (**12l**)*. Yield: 84%; white solid; ^{1}H NMR (600 MHz, DMSO-d_6): δ 8.76(s, 1H), 7.88–7.38 (m, 3H).

*2.2.5.13. 8-(Benzyloxy)-2-oxo-2H-chromene-3-carboxylic acid (**12m**)*. Yield: 92%; white solid; ^{1}H NMR (600 MHz, DMSO-d_6): δ 8.73 (s, 1H), 7.51–7.31 (m, 8H), 5.27 (s, 2H).

*2.2.5.14. 8-Methoxy-2-oxo-2H-chromene-3-carboxylic acid (**12n**)*. Yield: 94%; yellow solid; ^{1}H NMR (600 MHz, DMSO-d_6): δ 8.70 (s, 1H), 7.43–7.32 (m, 3H), 3.90 (s, 3H).

*2.2.5.15. 5,7-Dimethoxy-2-oxo-2H-chromene-3-carboxylic acid (**12o**)*. Yield: 90%; white solid; ^{1}H NMR (600 MHz, DMSO-d_6): δ 12.90 (s, 1H), 8.63 (s, 1H), 6.63–6.54 (m, 2H), 3.94 (s, 3H), 3.90 (s, 3H).

*2.2.5.16. 5,7-Di-tert-butyl-2-oxo-2H-chromene-3-carboxylic acid (**12p**)*. Yield: 79%; yellow solid; ^{1}H NMR (600 MHz, DMSO-d_6): δ 8.74(s, 1H), 7.81–7.65 (m, 2H), 1.56 (s, 9H), 1.32 (s, 9H).

*2.2.5.17. 7,8-Bis(benzyloxy)-2-oxo-2H-chromene-3-carboxylic acid (**12q**)*. Yield: 83%; yellow solid; ^{1}H NMR (600 MHz, DMSO-d_6): δ 8.70 (s, 1H), 7.66–7.28 (m, 12H), 5.31(s, 2H), 5.10 (s, 2H).

*2.2.5.18. 7,8-Dimethoxy-2-oxo-2H-chromene-3-carboxylic acid (**12r**)*. Yield: 64%; white solid; ^{1}H NMR (600 MHz, DMSO-d_6): δ 8.70 (s, 1H), 7.67–7.18 (m, 2H), 3.94 (s, 3H), 3.83 (s, 3H).

*2.2.5.19. 6,8-Dichloro-2-oxo-2H-chromene-3-carboxylic acid (**12s**)*. Yield: 91%; white solid; ^{1}H NMR (600 MHz, DMSO-d_6): δ 8.70 (s, 1H), 8.07–8.03 (m, 2H).

*2.2.5.20. 3-Oxo-3H-benzo[f]chromene-2-carboxylic acid (**12t**)*. Yield: 92%; green solid; ^{1}H NMR (600 MHz, DMSO-d_6): δ 9.27 (s, 1H), 8.51–8.02 (m, 3H), 7.74–7.52 (m, 3H).

*2.2.6. General synthetic procedure of compounds **13a–t***

To a solution of **9** (1.0 mmol) and **12** (1.2 mmol) in dry DCM (5 mL), DMAP (2.0 mmol) and EDCI (1.2 mmol) were added under an atmosphere of argon, and the mixture was allowed to stir for 24 h. Next, the resulting mixture was washed with 1M HCl (5 mL). The organic phases were dried, filtered, and evaporated in vacuo. Compounds **13b–t** were obtained by chromatography column (PE: EA = 10:1), but **13q** and **13r** were used directly in the next reaction without purification.

*2.2.6.1. 3,4-Bis(benzyloxy)phenethyl-2-oxo-2H-chromene-3-carboxylate (**13a**)*. Yield: 71%; white solid; ^{1}H NMR (600 MHz, $CDCl_3$): δ 8.44 (s, 1H), 7.65–7.28 (m, 13H), 6.94–6.79 (m, 3H), 5.16 (s, 2H), 5.14 (s, 2H), 4.48 (t, 2H, J = 6.6 Hz), 2.99 (t, 2H, J = 6.6 Hz).

*2.2.6.2. 3,4-Bis(benzyloxy)phenethyl-6-methyl-2-oxo-2H-chromene-3-carboxylate (**13b**)*. Yield: 81%; yellow solid; ^{1}H NMR (600 MHz, $CDCl_3$): δ 8.39 (s, 1H), 7.45–7.25 (m, 13H), 6.94–6.81 (m, 3H), 5.16 (s, 2H), 5.14 (s, 2H), 4.48 (t, 2H, J = 6.6 Hz), 2.99 (t, 2H, J = 6.6 Hz), 2.40 (s, 3H).

*2.2.6.3. 3,4-Bis(benzyloxy)phenethyl-6-chloro-2-oxo-2H-chromene-3-carboxylate (**13c**)*. Yield: 72%; yellow solid; ^{1}H NMR (600MHz, $CDCl_3$): δ 8.33 (s, 1H), 7.60–7.28

(m, 13H), 6.92–6.79 (m, 3H), 5.16 (s, 2H), 5.14 (s, 2H), 4.48 (t, 2H, *J* = 6.6 Hz), 2.98 (t, 2H, *J* = 6.6 Hz).

*2.2.6.4. 3,4-Bis(benzyloxy)phenethyl-6-hydroxy-2-oxo-2H-chromene-3-carboxylate **(13d)***. Yield: 81%; yellow solid; ^{1}H NMR (600 MHz, DMSO-d_6): δ 8.65 (d, 1H), 7.54–7.26 (m, 18H), 7.29–6.81 (m, 3H), 5.10 (s, 2H), 5.08 (s, 2H), 5.07 (s, 2H), 4.39 (t, 2H, *J* = 6.6 Hz), 2.91 (t, 2H, *J* = 6.6 Hz).

*2.2.6.5. 3,4-Bis(benzyloxy)phenethyl-6-methoxy-2-oxo-2H-chromene-3-carboxylate **(13e)***. Yield: 81%; yellow solid; ^{1}H NMR (600 MHz, DMSO-d_6): δ 8.67 (s, 1H), 7.45–7.28 (m, 13H), 7.10–6.82 (m, 3H), 5.08 (s, 2H), 5.07 (s, 2H), 4.39 (t, 2H, *J* = 6.6 Hz), 3.76 (s, 3H), 2.92 (t, 2H, *J* = 6.6 Hz).

*2.2.6.6. 3,4-Bis(benzyloxy)phenethyl-6-nitro-2-oxo-2H-chromene-3-carboxylate **(13f)***. Yield: 60%; white solid; ^{1}H NMR (600 MHz, DMSO-d_6): δ 8.94 (s, 1H), 8.93–7.65 (m, 3H), 7.42–7.28 (m, 10H), 7.12–6.84 (m, 3H), 5.09 (s, 2H), 5.08 (s, 2H), 4.43 (t, 2H, *J* = 6.6 Hz), 2.94 (t, 2H, *J* = 6.6 Hz).

*2.2.6.7. 3,4-Bis(benzyloxy)phenethyl-7-methyl-2-oxo-2H-chromene-3-carboxylate **(13g)***. Yield: 40%; white solid; ^{1}H NMR (600 MHz, DMSO-d_6): δ 8.67 (s, 1H), 7.76–7.22 (m, 13H), 7.09–6.81 (m, 3H), 5.08 (s, 2H), 5.07 (s, 2H), 4.38 (t, 2H, *J* = 6.6 Hz), 2.91 (t, 2H, *J*= 6.6 Hz), 2.43 (s, 3H).

*2.2.6.8. 3,4-Bis(benzyloxy)phenethyl-7-chloro-2-oxo-2H-chromene-3-carboxylate **(13h)***. Yield: 48%; White solid; ^{1}H NMR (600 MHz, DMSO-d_6): δ 8.73 (s, 1H), 7.92–7.83 (m, 10H), 7.09–6.81 (m, 3H), 5.08 (s, 2H), 5.07 (s, 2H), 4.39 (t, 2H, *J* = 6.6 Hz), 2.91 (t, 2H, *J* = 6.6 Hz).

2.2.6.9. 3,4-Bis(benzyloxy)phenethyl-7-hydroxy-2-oxo-2H-chromene-3-carboxylate ***(13i)***. Yield: 83%; white solid; ^{1}H NMR (600 MHz, DMSO-d_6): δ 8.67 (s, 1H), 7.81–6.81 (m, 18H), 5.24 (s, 2H), 5.08 (s, 2H), 5.07 (s, 2H), 4.36 (t, 2H, J = 6.6 Hz), 2.90 (t, 2H, J = 6.6 Hz).

2.2.6.10. 3,4-Bis(benzyloxy)phenethyl-7-methoxy-2-oxo-2H-chromene-3-carboxylate ***(13j)***. Yield: 65%; yellow solid; ^{1}H NMR (600 MHz, $CDCl_3$): δ 8.40(s, 1H), 7.45–7.27 (m, 13H), 6.94–6.79 (m, 3H), 5.15 (s, 2H), 5.12 (s, 2H), 4.46 (t, 2H, J = 6.6 Hz), 3.90 (s, 3H), 2.98 (t, 2H, J = 6.6 Hz).

2.2.6.11. 3,4-Bis(benzyloxy)phenethyl-8-methyl-2-oxo-2H-chromene-3-carboxylate ***(13k)***. Yield: 44%; white solid; ^{1}H NMR (600 MHz, DMSO-d_6): δ 8.70 (s, 1H), 7.72–7.10 (m, 13H), 6.99–6.83 (m, 3H), 5.09 (s, 2H), 5.08 (s, 2H), 4.30 (t, 2H, J = 6.6 Hz), 2.93 (t, 2H, J = 6.6 Hz), 2.37 (s, 3H).

2.2.6.12. 3,4-Bis(benzyloxy)phenethyl-8-chloro-2-oxo-2H-chromene-3-carboxylate ***(13l)***. Yield: 59%; white solid; ^{1}H NMR (600 MHz, DMSO-d_6): δ 8.74 (s, 1H), 7.89–7.28 (m, 13H), 7.27–6.82 (m, 3H), 5.08 (s, 2H), 5.07 (s, 2H), 4.40 (t, 2H, J = 6.6 Hz), 2.90 (t, 2H, J = 6.6 Hz).

2.2.6.13. 3,4-Bis(benzyloxy)phenethyl-8-hydroxy-2-oxo-2H-chromene-3-carboxylate ***(13m)***. Yield: 68%; yellow solid; ^{1}H NMR (600MHz, DMSO-d_6): δ 8.40 (s, 1H), 7.47–7.11 (m, 18H), 6.94–6.72 (m, 3H), 5.25 (s, 2H), 5.16 (s, 2H), 5.13 (s, 2H), 4.47 (t, 2H, J = 6.6 Hz), 2.98 (t, 2H, J = 6.6 Hz).

2.2.6.14. 3,4-Bis(benzyloxy)phenethyl-8-methoxy-2-oxo-2H-chromene-3-carboxylate ***(13n)***. Yield: 84%; yellow solid; ^{1}H NMR (600 MHz, DMSO-d_6): δ 8.69 (s, 1H),

7.43–7.11 (m, 13H), 6.99–6.83 (m, 3H), 5.10 (s, 1H), 5.09 (s, 1H), 4.40 (t, 2H, *J* = 6.6 Hz), 3.92 (s, 3H), 2.93 (t, 2H, *J* = 6.6 Hz).

*2.2.6.15. 3,4-Bis(benzyloxy)phenethyl-5,7-dimethoxy-2-oxo-2H-chromene-3-carboxylate (**13o**)*. Yield: 75%; white solid; ^{1}H NMR (600 MHz, $CDCl_3$): δ 8.78 (s, 1H), 8.64 (s, 1H), 7.44–7.28 (m, 10H), 6.94–6.81 (m, 3H), 6.41-6.26 (m, 2H), 5.15 (s, 1H), 5.13 (s, 1H), 4.45 (t, 2H, *J* = 7.2 Hz), 3.88 (s,6H) , 2.82 (t, 2H, *J* = 7.2 Hz).

*2.2.6.16. 3,4-Bis(benzyloxy)phenethyl-6,8-di-tert-butyl-2-oxo-2H-chromene-3-carboxylate (**13p**)*. Yield: 94%; white solid; ^{1}H NMR (600 MHz, $CDCl_3$): δ 8.45 (s, 1H), 7.68–7.26 (m, 12H), 7.27–6.81 (m, 3H), 5.17 (s, 2H), 5.14 (s, 2H), 4.48 (t, 2H, *J* = 7.2 Hz), 2.99 (t, 2H, *J* = 7.2 Hz), 1.53 (s, 9H), 1.35(s, 9H).

*2.2.6.17. 3,4-Bis(benzyloxy)phenethyl-6,8-dichloro-2-oxo-2H-chromene-3-carboxylate (**13s**)*. Yield: 78%; yellow solid; ^{1}H NMR (600 MHz, $CDCl_3$): δ 8.29 (s, 1H), 7.68–7.26 (m, 12H), 6.92–6.79 (m, 3H), 5.16 (s, 2H), 5.14 (s, 2H), 4.49 (t, 2H, *J* =7.2 Hz), 2.98 (t, 2H, *J* = 7.2 Hz).

*2.2.6.18. 3,4-Bis(benzyloxy)phenethyl-3-oxo-3H-benzo[f]chromene-2-carboxylate (**13t**)*. Yield: 77%; white solid; ^{1}H NMR (600 MHz, DMSO-d_6): δ 9.27 (s, 1H), 8.50–8.08 (m, 3H), 7.76–7.34 (m, 3H), 7.32-7.26 (m, 10H), 6.88–7.15 (m, 3H), 5.09 (s, 2H), 5.08 (s, 2H), 4.46 (t, 2H, *J* = 6.6 Hz), 2.99 (t, 2H, *J* = 6.6 Hz).

*2.2.7. General synthetic procedure of compounds **14a–t***

A solution of **13** (0.40 mmol) in dry DCM (2 mL) added 1M BBr_3 in DCM (2 mL) at -40℃ followed by stirring for 15 min. Next, the resulting mixture was added water to quench and extracted with ethyl acetate (10 mL×3). The combined organic extracts

were washed with saturated NaCl (10 mL), dried over Na_2SO_4, filtered, and evaporated in vacuo. The crude product was purified by column chromatography (DCM: MeOH= 100:1 to 50:1) to give target compounds **14a–t**.

*2.2.7.1. 3,4-Dihydroxyphenethyl-2-oxo-2H-chromene-3-carboxylate (**14a**)*. Yield: 50%; yellow powder; m.p.: 115–117 ℃; ^{1}H NMR (600 MHz, DMSO-d_6) δ 8.77 (brs, 2H), 8.68 (s, 1H), 7.90–7.40 (m, 3H), 6.69–6.55 (m, 3H), 4.35 (t, 2H, J = 6.6 Hz), 2.84 (t, 2H, J = 6.6 Hz); ^{13}C NMR (150 MHz, DMSO-d_6) δ 162.4, 155.9, 154.5, 148.6, 145.1, 143.8, 134.5, 130.2, 128.3, 124.8, 119.6, 117.7, 116.3, 116.1, 115.5, 66.0, 33.7; HRMS (ESI) *m/z*: Calcd for $C_{18}H_{14}O_6Na$ $[M+Na]^+$ 349.0688; found, 349.0697; HPLC purity = 96.08% (MeOH: H_2O = 85:15, 1 mL/min, t_R = 3.960 min).

*2.2.7.2. 3,4-Dihydroxyphenethyl-6-methyl-2-oxo-2H-chromene-3-carboxylate (**14b**)*. Yield: 78%; yellow powder; m.p.: 140–142 ℃; ^{1}H NMR (600 MHz, DMSO-d_6): δ 8.81 (d, 1H), 8.74 (s, 1H), 8.60 (s, 1H), 7.68–7.34 (m, 3H), 6.68–6.55 (m, 3H), 4.35 (t, 2H, J = 6.6 Hz), 2.82 (t, 2H, J = 6.6 Hz), 2.38 (s, 3H); ^{13}C NMR (150 MHz, DMSO-d_6) δ 162.4, 156.0, 152.7, 148.5, 145.1, 143.8, 135.4, 134.2, 129.6, 128.3, 119.6, 115.9, 115.6, 66.0, 33.7, 20.1; HRMS (ESI) *m/z* Calcd for $C_{19}H_{16}O_6Na$ $[M+Na]^+$ 363.0845; found, 363.0854; HPLC purity = 96.51% (MeOH: H_2O = 85:15, 1 mL/min, t_R = 4.280 min).

*2.2.7.3. 3,4-Dihydroxyphenethyl-6-chloro-2-oxo-2H-chromene-3-carboxylate (**14c**)*. Yield: 47%; yellow powder; m.p.: 178–180 ℃; ^{1}H NMR (600 MHz, DMSO-d_6): δ 8.80 (d, 1H), 8.74 (s, 1H), 8.66 (s, 1H), 8.05–7.48 (m, 3H), 6.68–6.55 (m, 3H), 4.36 (t, 2H, J = 6.6 Hz), 2.83 (t, 2H, J = 6.6 Hz); ^{13}C NMR (150 MHz, DMSO-d_6): δ 162.1, 155.4, 153.1, 147.3, 145.1, 143.8, 133.8, 129.0, 128.4, 128.2, 119.6, 119.1, 118.7, 118.2, 116.3,

115.5, 66.1, 33.6; HRMS (ESI) m/z: Calcd for $C_{18}H_{13}ClO_6Na$ $[M+Na]^+$ 383.0298; found, 383.0312; HPLC purity = 99.64% (MeOH: H_2O = 85:15, 1 mL/min, t_R = 4.389 min).

*2.2.7.4. 3,4-Dihydroxyphenethyl-6-hydroxy-2-oxo-2H-chromene-3-carboxylate (**14d**).* Yield: 54%; yellow powder; m.p.: 213–215 ℃; ^{1}H NMR (600 MHz, DMSO-d_6): δ 9.91 (s, 1H), 8.79 (s, 1H), 8.72 (s, 1H), 8.58 (s, 1H), 7.29–7.15 (m, 3H), 6.66–6.53 (m, 3H), 4.32 (t, 2H, *J* = 6.6 Hz), 2.81 (t, 2H, *J* = 6.6 Hz); ^{13}C NMR (150 MHz, DMSO-d_6): δ 162.6, 156.2, 154.0, 148.5, 147.9, 145.1, 143.8, 128.3, 122.7, 119.6, 118.2, 117.6, 117.1, 116.3, 115.6, 113.8, 67.0, 33.7; HRMS (ESI) m/z: Calcd for $C_{18}H_{14}O_7Na$ $[M+Na]^+$ 365.0637; found, 365.0650; HPLC purity = 95.72% (MeOH: H_2O = 85:15, 1 mL/min, t_R = 3.863 min).

*2.2.7.5. 3,4-Dihydroxyphenethyl-6-methoxy-2-oxo-2H-chromene-3-carboxylate (**14e**).* Yield: 54%; yellow powder; m.p.: 146–147 ℃; ^{1}H NMR (600 MHz, DMSO-d_6): δ 8.79 (d, 1H), 8.73 (s, 1H), 8.62 (s, 1H), 7.45–7.32 (m, 3H), 6.66–6.53 (m, 3H), 4.33 (t, 2H, *J* = 6.6 Hz), 3.81 (s, 3H), 2.81 (t, 2H, *J* = 6.6 Hz); ^{13}C NMR (150 MHz, DMSO-d_6): δ 162.6, 156.2, 155.8, 149.1, 148.6, 145.2, 143.9, 128.5, 122.5, 119.7, 118.2, 117.8, 117.4, 116.3, 115.7, 111.1, 66.1, 55.9, 33.8; HRMS (ESI) m/z: Calcd for $C_{19}H_{16}O_7Na$ $[M+Na]^+$ 379.0794; found, 379.0807; HPLC purity = 99.02% (MeOH: H_2O = 85:15, 1 mL/min, t_R = 4.177 min).

*2.2.7.6. 3,4-Dihydroxyphenethyl-6-nitro-2-oxo-2H-chromene-3-carboxylate (**14f**).* Yield: 45%; yellow powder; m.p.: 214–216 ℃; ^{1}H NMR (600 MHz, DMSO-d_6): δ 8.93 (d, 1H), 8.89 (s, 1H), 8.81 (s, 1H), 8.75 (s, 1H), 8.52–8.50 (m, 1H), 7.65 (d, 1H),

6.56–6.68 (m, 3H), 4.38 (t, 2H, J = 6.6 Hz), 2.84 (t, 2H, J = 6.6Hz); ^{13}C NMR (150 MHz, DMSO-d_6): δ 162.0, 158.1, 155.0, 147.7, 145.1, 143.9, 143.7, 128.6, 128.6, 126.1, 119.6, 119.4, 118.2, 117.8, 116.3, 115.6, 66.3, 33.7; HRMS (ESI) m/z: Calcd for $C_{18}H_{13}NO_8Na$ $[M+Na]^+$ 394.0539; found, 394.0552; HPLC purity = 95.51% (MeOH: H_2O = 85:15, 1 mL/min, t_R = 3.979 min).

2.2.7.7. 3,4-Dihydroxyphenethyl-7-methyl-2-oxo-2H-chromene-3-carboxylate ***(14g)***. Yield: 40%; yellow powder; m.p.: 165–168 ℃; ^{1}H NMR (600 MHz, DMSO-d_6): δ 8.79 (s, 1H), 8.72 (s, 1H), 8.63 (s, 1H), 7.77–7.23 (m, 3H), 6.66–6.53 (m, 3H), 4.32 (t, 2H, J = 6.6 Hz), 2.81 (t, 2H, J = 6.6 Hz), 2.43 (s, 3H); ^{13}C NMR (150 MHz, DMSO-d_6): δ 162.5, 156.0, 154.7, 148.7, 146.1, 145.1, 143.8, 130.0, 129.9, 128.3, 126.0, 119.5, 116.3, 116.3, 116.2, 115.6, 115.4, 66.9, 33.7, 21.5; HRMS (ESI) m/z: Calcd for $C_{18}H_{14}O_6Na$ $[M+Na]^+$ 363.0845; found, 363.0859; HPLC purity = 98.08% (MeOH: H_2O = 85:15, 1 mL/min, t_R = 4.266 min).

2.2.7.8. 3,4-Dihydroxyphenethyl-7-chloro-2-oxo-2H-chromene-3-carboxylate ***(14h)***. Yield: 60%; yellow powder; m.p.: 170–172 ℃; ^{1}H NMR (600 MHz, DMSO-d_6): δ 8.78 (s, 1H), 8.72 (s, 1H), 8.69 (s, 1H), 7.93–7.48 (m, 3H), 6.66–6.53 (m, 3H), 4.34 (t, 2H, J = 6.6Hz), 2.81 (t, 2H, J = 6.6 Hz); ^{13}C NMR (150 MHz, DMSO-d_6): δ 162.2, 155.3, 154.9, 148.0, 145.1, 143.8, 138.8, 131.6, 131.5, 128.3, 125.2, 119.6, 117.5, 116.8, 116.3, 115.6, 66.1, 33.7; HRMS (ESI) m/z: Calcd for $C_{18}H_{13}ClO_6Na$ $[M+Na]^+$ 383.0298; found, 383.0311; HPLC purity = 99.26% (MeOH: H_2O = 85:15, 1 mL/min, t_R = 4.504 min).

2.2.7.9. 3,4-Dihydroxyphenethyl-7-hydroxy-2-oxo-2H-chromene-3-carboxylate ***(14i)***.

Yield: 42%; yellow powder; m.p.: 202–204 ℃; ^{1}H NMR (600 MHz, DMSO-d_6): δ 11.12 (s, 1H), 8.81 (s, 1H), 8.74 (s, 1H), 8.60 (s, 1H), 6.74–7.55 (m, 6H), 4.32 (t, 2H, J = 7.2 Hz), 2.82 (t, 2H, J = 7.2 Hz); ^{13}C NMR (150 MHz, DMSO-d_6): δ 164.1, 162.7, 157.1, 156.3, 149.4, 145.1, 143.8, 132.1, 128.4, 119.6, 116.3, 115.5, 114.0, 111.9, 110.4, 101.8, 65.7, 33.8; HRMS (ESI) m/z: Calcd for $C_{18}H_{14}O_7Na$ $[M+Na]^+$ 365.0637; found, 365.0650; HPLC purity = 97.22% (MeOH: H_2O = 85:15, 1 mL/min, t_R = 3.530 min).

*2.2.7.10. 3,4-Dihydroxyphenethyl-7-methoxy-2-oxo-2H-chromene-3-carboxylate (**14j**)*. Yield: 48%; yellow powder; m.p.: 185–188 ℃; ^{1}H NMR (600 MHz, DMSO-d_6): δ 8.80 (s, 1H), 8.73 (s, 1H), 8.66 (s, 1H), 7.84–7.01 (m, 3H), 6.68–6.55 (m, 3H), 4.33 (t, 2H, J = 7.2 Hz), 3.90 (s, 3H), 2.82 (t, 2H, J = 7.2 Hz); ^{13}C NMR (150 MHz, DMSO-d_6): δ 164.8, 162.6, 157.0, 156.1, 149.1, 145.1, 143.8, 131.6, 128.3, 119.5, 116.3, 115.5, 113.3, 111.3, 110.3, 65.709, 56.2, 33.7; HRMS (ESI) m/z: Calcd for $C_{19}H_{16}O_7Na$ $[M+Na]^+$ 379.0794; found, 379.0807; HPLC purity = 96.96% (MeOH: H_2O = 85:15, 1 mL/min, t_R = 4.168 min).

*2.2.7.11. 3,4-Dihydroxyphenethyl-8-methyl-2-oxo-2H-chromene-3-carboxylate (**14k**)*. Yield: 67%; yellow powder; m.p.: 149–150 ℃; ^{1}H NMR (600 MHz, DMSO-d_6): δ 8.83 (s, 1H), 8.76 (s, 1H), 8.67 (s, 1H), 7.74–7.32 (m, 3H), 6.69–6.56 (m, 3H), 4.36 (t, 2H, J = 7.2 Hz), 2.84 (t, 2H, J = 7.2 Hz), 2.39 (s, 3H); ^{13}C NMR (150 MHz, DMSO-d_6): δ 162.5, 156.0, 152.8, 149. 0, 145.1, 143.8, 135.6, 128.4, 128.0, 125.1, 119.6, 117.5, 117.2, 116.4, 115.6, 66.0, 33.7, 14.8; HRMS (ESI) m/z: Calcd for $C_{19}H_{16}O_6Na$ $[M+Na]^+$ 363.0843; found, 363.0857; HPLC purity = 98.18% (MeOH: H_2O = 85:15, 1 mL/min, t_R = 4.374 min).

2.2.7.12. 3,4-Dihydroxyphenethyl-8-chloro-2-oxo-2H-chromene-3-carboxylate ***(14l)***. Yield: 46%; yellow powder; m.p.: 57–60 ℃; ^{1}H NMR (600 MHz, DMSO-d_6): δ 8.79 (s, 1H), 8.72 (s, 1H), 8.70 (s, 1H), 7.89–7.39 (m, 3H), 6.66–6.53 (m, 3H), 4.35 (t, 2H, J = 6.6 Hz), 2.82 (t, 2H, J = 6.6 Hz); ^{13}C NMR (150 MHz, DMSO-d_6): δ 162.1, 155.0, 149.9, 148.4, 145.1, 143.8, 134.2, 129.2, 128.3, 125.3, 119.6, 119.5, 119.4, 118.3, 116.3, 115.6, 66.2, 33.7; HRMS (ESI) m/z: Calcd for $C_{18}H_{13}ClO_6Na$ $[M+Na]^+$ 383.0298; found, 383.0311; HPLC purity = 97.18% (MeOH: H_2O = 85:15, 1 mL/min, t_R = 4.264 min).

2.2.7.13. 3,4-Dihydroxyphenethyl-8-hydroxy-2-oxo-2H-chromene-3-carboxylate ***(14m)***. Yield: 33%; yellow powder; m.p.: 178–181 ℃; ^{1}H NMR (600MHz, DMSO-d_6): δ 10.40 (s, 1H), 8.81 (s, 1H), 8.74 (s, 1H), 8.61 (s, 1H), 7.32–7.22 (m, 3H), 6.68–6.55 (m, 3H), 4.35 (t, 2H, J= 7.2 Hz), 2.84 (t, 2H, J = 7.2 Hz); ^{13}C NMR (150 MHz, DMSO-d_6): δ 162.5, 155.8, 149.1, 145.1, 144.4, 143.8, 143.2, 128.3, 124.8, 120.6, 120.1, 119.6, 118.6, 117.4, 116.3, 115.5, 66.0, 33.7. HRMS (ESI) m/z: Calcd for $C_{18}H_{14}O_7Na$ $[M+Na]^+$ 365.0637; found, 365.0649; HPLC purity = 95.42% (MeOH: H_2O = 85:15, 1 mL/min, t_R = 3.948 min).

2.2.7.14. 3,4-Dihydroxyphenethyl-8-methoxy-2-oxo-2H-chromene-3-carboxylate ***(14n)***. Yield: 40%; yellow powder; m.p.: 90–92 ℃; ^{1}H NMR (600 MHz, DMSO-d_6): δ 8.82 (s, 1H), 8.75 (s, 1H), 8.65 (s, 1H), 7.44–7.34 (m, 3H), 6.69–6.56 (m, 3H), 4.36 (t, 2H, J = 7.2 Hz), 3.93 (s, 3H), 2.84 (t, 2H, J = 7.2 Hz); ^{13}C NMR (150 MHz, DMSO-d_6): δ 162.4, 155.6, 148.9, 146.2, 145.1, 143.8, 128.3, 124.8, 121.1, 119.6, 118.235, 117.7, 116.5, 116.3 115.6, 79.1, 66.0, 56.4, 33.7; HRMS (ESI) m/z: Calcd for

$C_{19}H_{16}O_7Na$ $[M+Na]^+$ 379.0794; found, 379.0806; HPLC purity = 97.71% (MeOH: H_2O = 85:15, 1 mL/min, t_R = 4.001 min).

2.2.7.15. 3,4-Dihydroxyphenethyl-5,7-dimethoxy-2-oxo-2H-chromene-3-carboxylate ***(14o)***. Yield: 54%; yellow powder; m.p.: 192–195 ℃; ^{1}H NMR (600 MHz, DMSO-d_6): δ 8.78 (s, 1H), 8.73 (s, 1H), 8.57 (s, 1H), 6.67–6.64 (m, 3H), 6.55–6.54 (m, 2H), 4.31 (t, 2H, J = 7.2 Hz), 3.95 (s, 3H), 3.90 (s, 3H), 2.80 (t, 2H, J = 7.2 Hz); ^{13}C NMR (150 MHz, DMSO-d_6): δ 166.4, 162.4, 158.2, 157.6, 156.1, 145.1, 143.8, 134.5, 128.4, 119.6, 116.2, 115.5, 95.2, 93.0, 65.5, 56.6, 56.3, 33.7; HRMS (ESI) m/z: Calcd for $C_{20}H_{18}O_8Na$ $[M+Na]^+$ 409.0899; found, 409.0911; HPLC purity = 95.53% (MeOH: H_2O = 85:15, 1 mL/min, t_R = 4.351 min).

2.2.7.16. 3,4-Dihydroxyphenethyl-6,8-di-tert-butyl-2-oxo-2H-chromene-3-carboxylate ***(14p)***. Yield: 48%; yellow powder; m.p.: 70–73 ℃; ^{1}H NMR (600 MHz, DMSO-d_6): δ 8.80 (s, 1H), 8.73 (s, 1H), 8.70 (s, 1H), 7.80–7.66 (m, 2H), 6.70–6.57 (m, 3H), 4.35 (t, 2H, J = 7.2 Hz), 2.84 (t, 2H, J = 7.2 Hz), 1.46 (s, 9H), 1.34 (s, 9H); ^{13}C NMR (150 MHz, $CDCl_3$): δ 163.4, 157.4, 152.0, 150.9, 147.9, 143.9, 142.9, 137.5, 130.1, 124.2, 121.1, 117.9, 116.2, 115.3, 66.6, 35.1, 34.7, 34.4, 31.2, 29.7; HRMS (ESI) m/z: Calcd for $C_{26}H_{30}O_6$ $[M+Na]^+$ 461.1952; found, 461.1940; HPLC purity = 95.74% (MeOH: H_2O = 85:15, 1 mL/min, t_R = 8.871 min).

2.2.7.17. 3,4-Dihydroxyphenethyl-7,8-dihydroxy-2-oxo-2H-chromene-3-carboxylate ***(14q)***. Yield: 52%; yellow powder; m.p.: 228–230 ℃; ^{1}H NMR (600 MHz, DMSO-d_6): δ 8.54 (s, 1H), 6.54–6.24 (m, 2H), 4.31 (t, 2H, J = 6.6 Hz), 2.82 (t, 2H, J = 6.6 Hz); ^{13}C NMR (150 MHz, DMSO-d_6): δ 162.8, 156.3, 152.9, 149.9, 145.1, 144.9, 143.8, 131.8,

128.4, 121.6, 119.6, 116.3, 115.5, 13.3, 111.5, 111.0, 65.6, 33.7; HRMS (ESI) m/z: Calcd for $C_{18}H_{14}O_8Na$ $[M+Na]^+$ 381.0586; found, 381.0601; HPLC purity = 98.07% (MeOH: H_2O = 85:15, 1 mL/min, t_R = 3.542 min).

2.2.7.18. 3,4-Dihydroxyphenethyl-7,8-dimethoxy-2-oxo-2H-chromene-3-carboxylate ***(14r)***. Yield: 43%; yellow powder; m.p.: 141–144 ℃; ^{1}H NMR (600 MHz,DMSO-d_6): δ 8.80 (s, 1H), 8.73 (s, 1H), 8.64 (s, 1H), 7.67–7.19 (m, 2H), 6.68–6.55 (m, 3H), 4.33 (t, 2H, J =7.2 Hz), 3.95 (s, 3H), 3.83 (s, 3H), 2.82 (t, 2H, J = 7.2 Hz); ^{13}C NMR (150 MHz, DMSO-d_6): δ 162.7, 157.6, 155.9, 149.4, 148.5, 145.1, 143.8, 134.8, 128.5, 126.2, 119.7, 116.4, 115.6, 113.7, 112.5, 110.0, 65.9, 60.9, 65.7, 33.8; HRMS (ESI) m/z: Calcd for $C_{20}H_{18}O_8Na$ $[M+Na]^+$ 409.0899; found, 409.0911; HPLC purity = 95.84% (MeOH: H_2O = 85:15, 1 mL/min, t_R = 3.917 min).

2.2.7.19. 3,4-Dihydroxyphenethyl-6,8-dichloro-2-oxo-2H-chromene-3-carboxylate ***(14s)***. Yield: 67%; yellow powder; m.p.: 218–222 ℃; ^{1}H-NMR (600 MHz, DMSO-d_6): δ 8.77 (s, 1H), 8.71 (s, 1H), 8.65 (s, 1H), 8.06–8.02 (m, 2H), 6.67–6.54 (m, 3H), 4.36 (t, 2H, J = 7.2 Hz), 2.82 (t, 2H, J = 7.2 Hz); ^{13}C NMR (150 MHz, DMSO-d_6): δ 162.5, 155.9, 155.1, 145.2, 143.9, 136.1, 129.7, 129.1, 128.990, 128.9, 128.5, 126.4, 121.9, 119.6, 116.4, 116.3, 115.5, 111.7, 65.9, 33.7; HRMS (ESI) m/z: Calcd for $C_{18}H_{12}Cl_2O_6Na$ $[M+Na]^+$ 416.9909; found, 416.9922; HPLC purity = 96.78% (MeOH: H_2O = 85:15, 1 mL/min, t_R = 4.852 min).

2.2.7.20. 3,4-Dihydroxyphenethyl-3-oxo-3H-benzo[f]chromene-2-carboxylate ***(14t)***. Yield: 52%; yellow powder; m.p.: 187–190℃; ^{1}H NMR (600 MHz, DMSO-d_6): δ 9.25 (s, 1H), 8.82 (s, 1H), 8.77 (s, 1H), 8.48–8.08 (m, 3H), 7.84–7.58 (m, 3H), 6.60–6.74

(m, 3H), 4.41 (t, 2H, J = 6.6 Hz), 2.89 (t, 2H, J = 6.6 Hz); ^{13}C NMR (150 MHz, DMSO-d_6): δ 162.5, 155.9, 155.2, 145.2, 143.9, 136.1, 129.7, 129.1, 129.0, 128.9, 128.5, 126.4, 121.9, 119.6, 116.4, 116.3, 115.5, 111.7, 65.9, 33.7; HRMS (ESI) m/z: Calcd for $C_{22}H_{16}O_6Na$ $[M+Na]^+$ 399.0845; found, 399.0856; HPLC purity = 96.20% (MeOH: H_2O = 85:15, 1 mL/min, t_R = 4.513 min).

2.3. Antioxidant assays

2.3.1. Cell survival conditions

HepG2 WI-38 cells obtained from General Hospital of Lanzhou Military Command were grown at 37℃ in DMEM supplemented with 10% fetal bovine serum, and 1% penicillin/streptomycin in a humidified atmosphere containing 5% CO_2. The medium was replaced once every second day. All materials were obtained from commercial suppliers (Solarbio and Beyotime Biotechnology). Each of the experiments was done in triplicate and the mean value of each reading was reported within.

2.3.2. Free radical scavenging assay

2.3.2.1. DPPH radical scavenging assay

1,1-Diphenyl-2-picrylhydrazyl (DPPH) radical scavenging activities of all the synthesized compounds **14a**–**t**, **1**, and **3** were examined by DPPH assay [24]. Butylated hydroxytoluene (BHT) was used as the standard. DPPH was prepared into a 10 mM stock solution with ethanol to produce DPPH free radicals, and then diluted with ethanol. 100 μL of various concentration solutions of compounds **14a**–**t**, **1**, and **3** in methanol was mixed with 100 μL of 0.5 mM DPPH• solution in a 96-well plate, then

the mixture was incubated at 25 ℃ for 1 h in the dark. The absorbance was measured at 517 nm using a spectrophotometer. The antiradical activity was calculated as IC_{50} according to % scavenged [DPPH•].

% scavenged [DPPH•] = [(Absorbance of control–Absorbance of sample)/Absorbance of control] × 100

2.3.2.2. ABTS radical cation scavenging assay

The 2,2'-azino-di(3-ethylbenzthiazoline sulphonate) (ABTS) radical cation scavenging activities of all the synthesized compounds **14a**–**t**, **1**, and **3** were examined using ABTS assay [24]. Distilled water (10 mL) was prepared into a mixed solution of ABTS salt (4 mM) and $K_2S_2O_8$ (1.41 mM), and placed in the dark at 25℃ for 24h to form $ABTS^{+\bullet}$ free radicals, then diluted with 100mL of ethanol. 50 μL of various concentration solutions of compounds **14a–t**, **1**, and **3** in methanol were added to the 96-well plate, 150 μL of $ABTS^{+\bullet}$ solution was added, and incubated at 25℃ for 10 min in the dark. The absorbance was measured at 734 nm. The antiradical activity was calculated as IC_{50} according to %scavenged [$ABTS^{+\bullet}$].

% scavenged [$ABTS^{+\bullet}$] = [(Absorbance of control – Absorbance of sample)/Absorbance of control] × 100

2.3.3. Cytotoxic assay

2.3.3.1. Hemolysis assay

The toxicity was evaluated on 5% (v/v) suspension of rat RBCs in PBS (control). After 2 h of RBCs hemolysis incubated with different concentrations (200, 100, 50, and

25 μM) of test compounds (**14d**, **14i**, **14m**, **14q**, **3**, **1**, and BHT), incubation liquids were centrifuged for 5 min (10000 r/min). Hemolysis was determined as hemoglobin content in the supernatant at λ 540 nm. The H_2O-treated controls were assigned a hemolysis of 100%.

2.3.3.2. Cytotoxic assay in human normal cells line WI-38 and GES by MTT

Cells were plated in 96-well plates at a density of 5×10^3 cells per well in 100 μL medium. After 24 h incubation, compounds **14d**, **14i**, **14m**, **14q**, **3**, **1**, and BHT (200, 100, 50, 25 and 12.5 μM) were added to each well and incubated for 48 h. After attached cells were incubated with 5 mg/mL (Sigma, USA) for another 4 h, the suspension was solubilized in dimethyl sulfoxide (DMSO). The absorbance of the 490 nm was measured using a multifunction microplate reader (Molecular Devices, Flex Station 3). The DMSO-treated controls were assigned negative control.

2.3.4. Cell viability assay in H_2O_2-damaged WI-38 and HepG2 cells by MTT

HepG2 cells were plated in 96-well plates at a density of 5×10^3 cells per well in 100 μL medium. After 24 h incubation, compound **14q** (50, 25 and 12.5 μM) was added to each well and incubated for 1 h. Subsequently, H_2O_2 (400 μM) was added and cells were incubated for 12 h to induce cell injury. MTT assay was performed as mentioned above. The no compound-treated controls were assigned a cell viability value of 100%. Cell viability (%) = OD value (sample group) / OD value (blank control) × 100%.

2.3.5. Apoptosis assay in H_2O_2-damaged HepG2 cells

Cells apoptosis was assayed by the Annexin-V-FITC Apoptosis Detection Kit (BD

Biosciences, USA) according to the manufacturer's instructions. Briefly, HepG2 cells were plated in 6-well plates at a density of 1×10^6 cells per well in 4 mL medium. After 24 h incubation, compounds **14q** (50, 25, 5 and 0 μM) were added to well and incubated for 1 h. Subsequently, H_2O_2 (400 μM) was added and cells were incubated for 12 h to induce cell injury. Damaged HepG2 cells were harvested, washed twice with ice-cold PBS, and resuspended in 1× binding buffer at a concentration of 1×10^6 cells/ mL. Subsequently, the cells were stained with 5 μL Annexin-V-FITC and 5 μL PI (50 mg/mL) for 10 min in the dark at 25℃, and analyzed by flow cytometry. The no H_2O_2-treated were assigned control.

2.3.6. ROS level assay

ROS level assay was measured at 488 excitation wavelength and 525 emission wavelength using reactive oxygen species assay kit (Beyotime Biotechnology S0033) by fluorescence spectrophotometer (RF-5301PC, Japan, Takatsu). HepG2 cells were plated in 6 cm dishes at a density of 1.0×10^6 cells per dish in 4 mL medium. After 24h incubation, compounds **14q** (50, 25, 5 and 0 μM) were added to each dish and incubated for 1 h. Subsequently, H_2O_2 (400 μM) was added and cells were incubated for 12 h to induce cell injury. ROS level was measured according to the manufacturer's instructions. The no H_2O_2-treated were assigned control.

2.3.7. LDH, SOD, and GSH level assay

HepG2 cells were plated in 6 cm dishes at a density of 1.0×10^6 cells per dish in 4 mL medium. After 24 h incubation, compounds **14q** (50, 25, 5 and 0 μM) were added

to each dish and incubated for 1 h. Subsequently, H_2O_2 (400 μM) was added and cells were incubated for 12 h to induce cell injury. LDH level was measured at 450 nm by LDH assay kit (Beijing Solarbio BC0680), SOD level was measured at 560 nm by SOD assay kit (Beijing Solarbio BC0170), and GSH level was measured at 405 nm based on the rate of oxidation of reduced glutathione to oxidized glutathione by reduced glutathione assay kit **(**Beijing Solarbio BC1175**)**. Their levels were measured according to the manufacturer's instructions. The no H_2O_2-treated were assigned control.

2.3.8. Stability assay

Compound **14q** and hydroxytyrosol were completely dissolved in methanol, and stored in 25℃or 50℃ for 0, 0.5, 1, 2, 4 and 6 days. The contents of compound **14q** and hydroxytyrosol contents were measured by HPLC (MeOH: H_2O= 80:20, 1 mL /min, LC-100HP, Wufeng, China), and expressed with their remaining percentage.

3. Results and discussion

Twenty new target compounds were synthesized as described in the Materials and Methods, and their structures were elucidated by ^{1}H NMR, ^{13}C NMR (see Supplementary data) and high resolution mass spectrometry, all spectral data were in accordance with assumed structures. The purities of synthesized target compounds were all above 95% by HPLC method.

The antioxidant capacity of the target conjugates **14a**–**t** were tested using two different methods, namely, the DPPH radical and ABTS radical cation scavenging assays [24]. BHT, hydroxytyrosol and coumarin were used as a positive control, the

IC_{50} values are summarized in Table 1. Generally, compounds **14a**–**t** displayed more potent DPPH radicals scavenging activity with IC_{50} values of 26.58 to 102.08 μM, compared with that of BHT, hydroxytyrosol and coumarin were 521.91, 143.81 and >10000 μM, respectively. It could be concluded that coumarin has no radical scavenging activity. However, the DPPH• scavenging activity of **14a** was 1.76 times of hydroxytyrosol, improved from 143.81 μM to 81.53 μM. Simultaneously, the DPPH radical scavenging activities of **14a**–**t** were changed with the different groups on the coumarin skeleton. Specifically, introduction of electron-withdrawing groups (*eg.* OH, Cl, or NO_2) at coumarin ring increased the antioxidant capacity (**14c**, **14d**, **14f**, **14h**, **14i**, **14l**, and **14m** *vs* **14a**). Especially, the multiple introduction of hydroxyl superimposed their scavenging activity of DPPH radical. On the contrary, the electron-donating groups (*eg.* Me, or OMe) at the coumarin ring reduced their antioxidant ability. The results confirmed the previous finding about the importance of hydroxyl group for the antioxidant property [25].

Table 1

Antioxidant activity of compounds **14a–t**

Compounds	R	DPPH• scavenging		$ABTS^{+\bullet}$ scavenging	
		IC_{50} (μM) [a]	Fold [b]	IC_{50} (μM) [a]	Fold [b]
14a	H	81.53±3.20	6.40	108.26±3.25	1.17
14b	6-CH_3	76.14±1.39	6.86	137.46±4.60	0.92
14c	6-Cl	71.36±1.02	7.31	124.14±1.71	1.02
14d	6-OH	70.06±2.54	7.45	78.88±4.23	1.61
14e	6-OCH_3	76.40±2.17	6.83	125.16±1.93	1.02

14f	6-NO_2	71.31±1.46	7.32	133.68±2.46	0.95
14g	7-CH_3	85.29±10.20	6.12	139.06±8.26	0.91
14h	7-Cl	79.87±3.78	6.54	143.83±3.83	0.88
14i	7-OH	78.16±1.94	6.68	124.50±7.03	1.02
14j	7-OCH_3	79.54±2.65	6.56	132.06±2.09	0.96
14k	8-CH_3	78.93±2.84	6.61	129.04±2.25	0.98
14l	8-Cl	77.64±1.40	6.72	139.30±3.41	0.91
14m	8-OH	71.32±3.95	7.32	105.40±8.24	1.21
14n	8-OCH_3	102.08±1.88	5.11	244.51±1.26	0.52
14o	5,7-OCH_3	82.86±5.24	6.30	145.68±4.49	0.87
14p	6,8-$C(CH_3)_3$	91.01±2.48	5.74	164.22±3.81	0.77
14q	7,8-OH	26.58±3.01	19.64	30.31±0.97	4.19
14r	7,8-OCH_3	92.05±1.58	5.67	194.61±1.81	0.65
14s	6,8-Cl	66.78±3.79	7.82	103.85±5.68	1.22
14t	5,6-phenyl ring	69.07±2.06	7.56	152.64±2.96	0.83
1	—	143.81±5.29	3.63	170.47±5.28	0.75
3	—	>10000	—	>10000	—
BHT	—	521.99±14.66	1.00	127.07±0.40	1.00

[a] IC_{50} is the concentration of scavenging 50% free radical.

[b] Fold = IC_{50} of BHT/IC_{50} of compounds **14a**–**t**.

In the $ABTS^{+\bullet}$ scavenging assay, the majority of target compounds **14a**–**t** (except **14n** and **14r**) also showed better activity with IC_{50} values ranging from 30.31 to 164.22 μM compared with hydroxytyrosol (170.47 μM) and coumarin (>10000 μM). The result of $ABTS^{+\bullet}$ scavenging assay also indicated that **14a** was more active than coumarin. Coincidentally, **14a** increased $ABTS^{+\bullet}$ scavenging activity compared with hydroxytyrosol, and substitution of different groups at the coumarin would also cause changes in $ABTS^{+}$ radical scavenging activity. Their $ABTS^{+\bullet}$ scavenging activity were

reduced when the hydrogen of coumarin ring was replaced by methyl group (**14b**, **14g**, and **14k**), chlorine group (**14c**, **14h**, and **14l**), or methoxyl (**14e**, **14j**, **14n**, and **14r**). However, the substitution with the hydroxyl group improved the $ABTS^{+\bullet}$ scavenging activity (**14d**, **14i** and **14m**), especially compounds **14q** had a superimposed effect with the IC_{50} value of 30.31±0.97 μM. It indicated that hydroxyl was important for increasing the antioxidant activity of conjugates. This suggestion was consistent with the DPPH radical scavenging results.

Based on the outstanding scavenging of free radical, compounds **14d**, **14i**, **14m**, and **14q** deserved further toxicity studies. The toxicity of representative compounds (**14d**, **14i**, **14m**, and **14q**) were evaluated by hemolysis assay and cytotoxicity assay in normal WI-38 (Human embryonic lung cells) and GES (Human gastric mucosal cells) cells [26]. As shown in Fig. 3, H_2O caused hemolysis of rat RBCs completely, the hemolysis of synthetic antioxidant BHT was slight at low concentrations (< 100 μM), yet severe (50.24%) at high concentration (200 μM). However, the selected compounds, especially for **14m** and **14q**, showed less hemolysis than the negative control (in 0.1M PBS), at either high or low concentrations (25–200 μM).

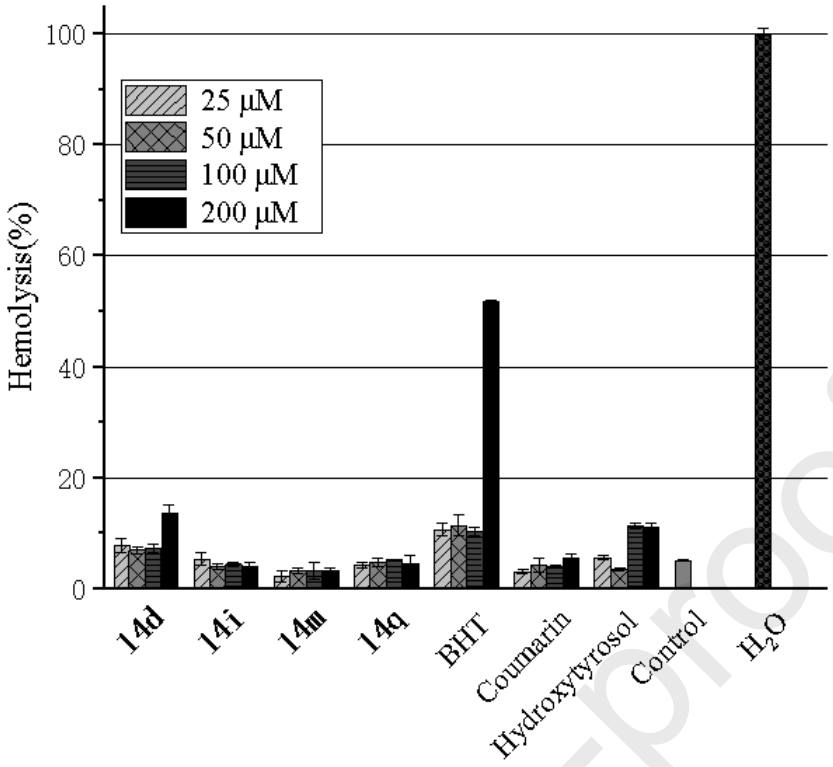

Fig. 3. Hemolysis of tested compounds. The H_2O-treated controls were assigned a hemolysis of 100%. All data are presented as means ± SD, n=3.

In cytotoxicity assay, all of compounds **14d**, **14i**, **14m**, and **14q** showed low cytotoxicity in human normal WI-38 (IC_{50} > 100 μM) and GES (IC_{50} > 200 μM) cells as shown in Table 2. The cytotoxicity of compounds followed the order: **14d** >BHT >**14i** >**14m** >**14q**. Especially, compound **14q**, with the IC_{50} values are more than 200 μM in both of WI-38 and GES cell lines, showed the least toxicity in these four conjugates. Thence, compound **14q** was selected to explore the antioxidant mechanism for its better antioxidant properties and less toxicity.

Table 2

Cytotoxicity of selected compounds

	IC_{50} (μM) [a]

Compounds	WI-38	GES
14d	106.87±7.60	>200
14i	123.18±3.91	>200
14m	144.17±23.43	>200
14q	>200	>200
BHT	122.36±8.17	>200
1	>200	>200
3	>200	>200

[a] All data are presented as means ±SD, n=3.

H_2O_2 stimulation caused oxidative stress and damage of biomacromolecules, such as nucleic acids, membrane lipids and proteins in cells [27], and had been extensively employed to induce cellular oxidative injury for further assessment of antioxidant activities [28]. The effects of **14q** in cell viability of tumor HepG2 (Human liver hepatocellular carcinoma) and normal WI-38 cells were investigated using MTT assay by Teng' method [29]. As shown in Fig. 4A, after 1 h of cell incubation with various concentrations of **14q** (0, 12.5, 25 and 50 μM) and treatment with 400 μM H_2O_2 for 12 h, the viability of H_2O_2-treated HepG2 cells declined to 33.85%. In contrast, the viability of HepG2 cells increased to 69.57%, 77.51% and 98.70% in treatment with **14q** at 12.5, 25 and 50 μM, respectively. Besides, **14q** also exhibited good cell viability effect to normal WI-38 cells as shown in Fig. 4B. H_2O_2-treated WI-38 cells declined to 51.71%, while those of **14q**-treated were improved to 91.71%, 101.35% and 99.2% at 12.5, 25 and 50 μM, respectively. These results suggested that compound **14q** could increase cells viability of H_2O_2-indcued cells and protected the H_2O_2-indcued cells

against injury, which was in accordance with previous publication that alkylresorcinols could play anti-oxidant effects and improves cell viability [30].

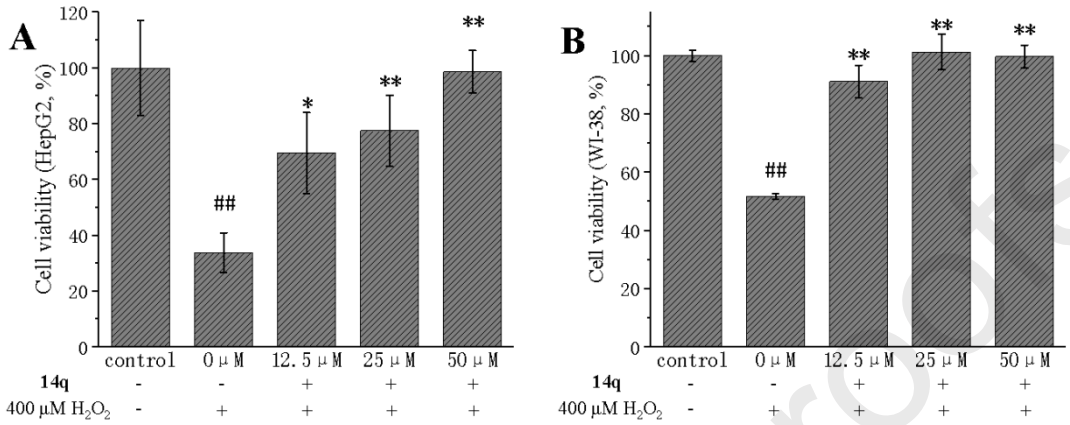

Fig. 4. The effects of **14q** in H_2O_2-induced cells viability. A) H_2O_2-induced HepG2 cells treated with **14q**. B) H_2O_2-induced WI-38 cells treated with compound **14q**. The DMSO-treated controls were assigned a cell viability value of 100%. All data are presented as means ± SD, n=3. $^{\#\#}P < 0.001$ compared to control cells; $*P < 0.01$, $**P < 0.001$ compared to H_2O_2-treated cells.

Apoptosis is one of the ways that oxidative stress leads to a decrease in cell viability [27,29]. To test whether compound **14q** has anti-apoptotic effects in H_2O_2-induced model, the morphological alterations of H_2O_2-injured HepG2 cells treated or untreated with compound **14q** were evaluated by double-labeled with Annexin V-FITC and propidium iodide (PI) and analyzed with flow cytometry [31]. The apoptotic rate of **14q** untreated H_2O_2-damaged HepG2 cells was 20.90%, while those of compound **14q** (5, 25 and 50 μM) treated cells obviously were declined to 9.32%, 8.95%, and 8.11% (Fig. 5). These results suggested that compound **14q** could protect the H_2O_2-injured HepG2 cells against apoptosis through antioxidant effect agreed with Du's result that polyphenols was proven to protect cardiac cells from apoptosis [32].

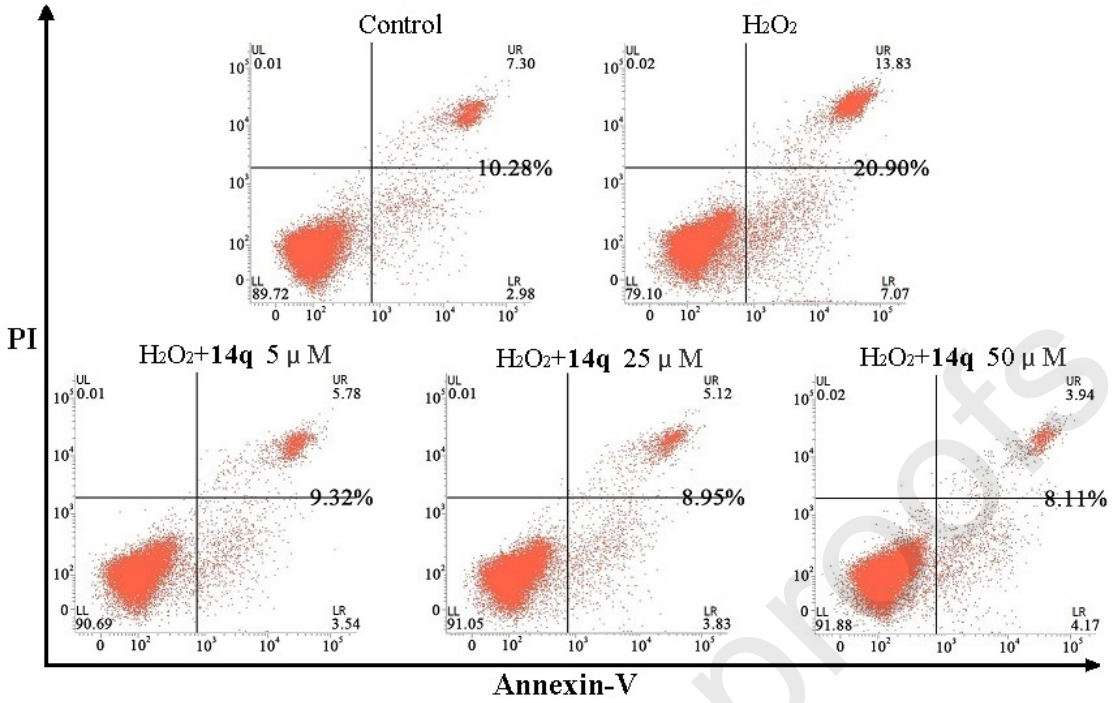

Fig. 5. The effects of compound **14q** on apoptosis in H_2O_2-injured HepG2 cells. The control was treated with 0.5% DMSO.

Except inducing cell apoptosis, cell oxidation caused a large accumulation of ROS in cells [33]. ROS caused damage to cells and represented an early step on apoptosis in many cell systems at high oxidative levels [34]. Thus, we employed DCFH-DA assay[35], an oxidation-sensitive fluorescent probe, to assess if it will play an anti-oxidant effect by reducing ROS. The fluorescence intensity showed that H_2O_2 could significantly increase the ROS level in HepG2 cells to 1.29-fold compared with the control group. The level of ROS in H_2O_2-induced HepG2 cells dealt with at 5, 25 and 50 μM was declined 11.23%, 15.14%, and 16.43% compared with H_2O_2-induced group, respectively (Fig. 6). The results indicated that **14q** could effectively decrease the H_2O_2-induced ROS level and provide a protective effect in cells against oxidative stress. This suggestion agreed with Kundu's research that ROS was effectively scavenged and

inhibited to induce antioxidant effect [36].

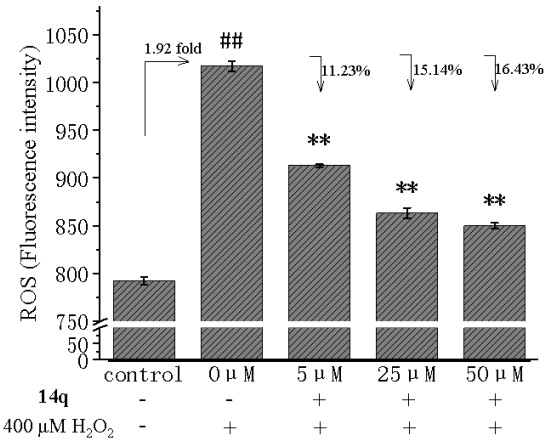

Fig. 6. ROS level in H_2O_2-induced HepG2 cells. The control was treated 0.5% DMSO. All data are presented as means ± SD, n=3. $^{\#\#}$ $P < 0.001$ compared to control cells; *$P < 0.01$, **$P < 0.001$ compared to H_2O_2-treated cells.

Owing to the generation of free radicals, oxidative stress causes accumulated oxidative damage to critical biomolecules, especially when coupled with an insufficient endogenous antioxidant defense mechanism [34]. To reveal the protective effects and antioxidant mechanism of compound **14q**, we evaluated the effects of **14q** on the release of lactate dehydrogenase (LDH), the levels of superoxide dismutase (SOD) and glutathione (GSH) in H_2O_2-induced HepG2 mode [29].

Cellular oxidative stress caused membrane lipid peroxidation with increasing the release of LDH in medium [38]. Therefore, evaluating the level of LDH was a way to illustrate the oxidation degree in H_2O_2-injured HepG2 cells [39]. As shown in Fig. 7A, HepG2 cells were exposed to H_2O_2 showed a higher LDH release level (27.86 U/mL) than that of normal cells (9.88 U/mL). Furthermore, **14q** could significantly attenuate the LDH release in cells per-treated with **14q**. The LDH content in supernatants treated with **14q** was 5.29 to 18.07 U/mL, which decreased greatly by 35.2–80.1% comparing

with H_2O_2-induced group. In addition, compound **14q** displayed the inhibition rate of 81.5% or 80.1% on LDH release at 25 or 50 μM. The results indicated that H_2O_2 induced HepG2 cells to serious membrane injury, and the **14q** had the capacity to repair and protect cells from H_2O_2-induced oxidative damage. This was similar to the desmethylxanthohumol analogs could act as antioxidants to repair damaged membrane and reduce LDH levels [29].

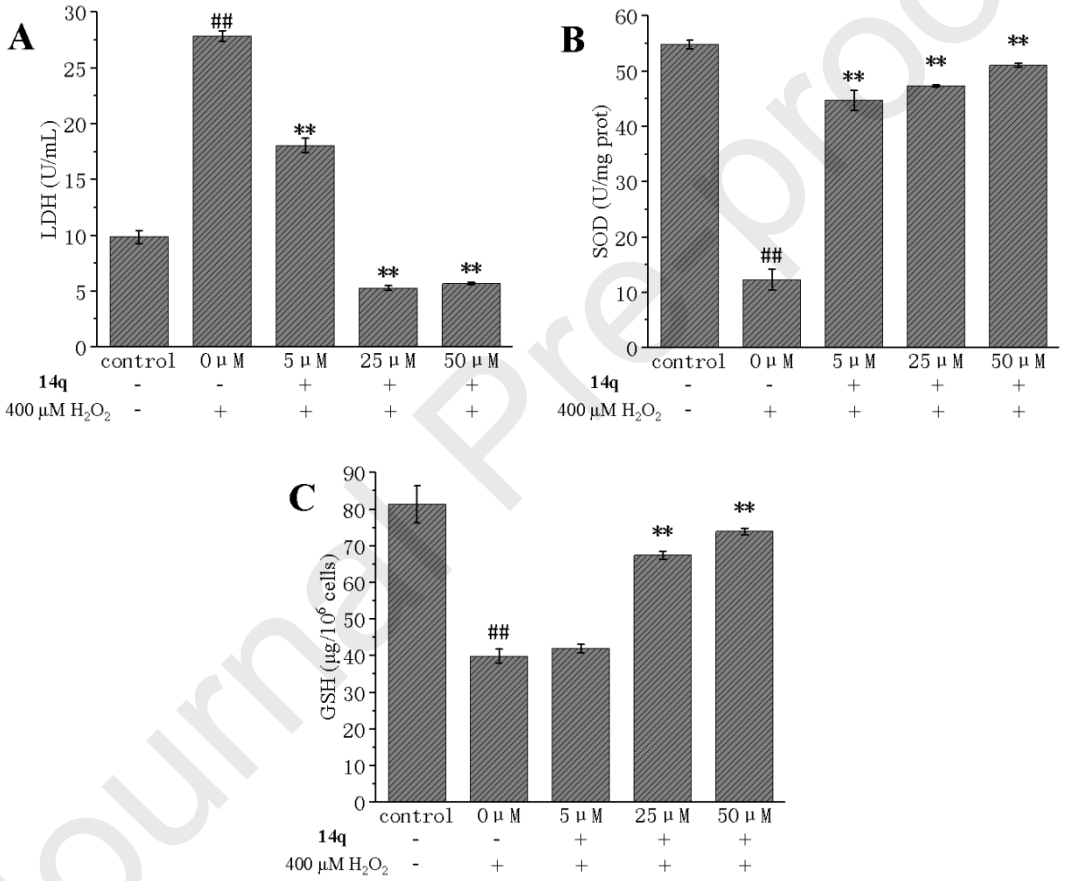

Fig. 7. Effects of compound **14q** on the release of LDH (A), the generation of SOD (B), and production of GSH (C) in H_2O_2-injured HepG2 cells. All data are presented as means ± SD, n=3. $^{\#\#}P < 0.001$ compared to control cells; $^{*}P < 0.01$, $^{**}P < 0.001$ compared to H_2O_2-treated cells.

SOD plays an essential role in the metabolism of $O_2^{\cdot -}$, and forestalls the oxidative chain reactions that cause inimical and unfavorable damage by preventing the cascade

of detrimental ROS [40]. Thence, the level of SOD was evaluated as an antioxidant state in H_2O_2-treated HepG2 cells [41]. As observed in Fig. 7B, H_2O_2-treated HepG2 cells showed only 22.4% of SOD activity (12.30 U/mg prot) compared with the normal ones (54.79 U/mg prot). However, compound **14q** showed a pronounced influence on oxidative stress of H_2O_2-treated HepG2 cells, and promoted the production of SOD in a dose-dependent manner. With increasing **14q** from 5 to 50 μM, the corresponding SOD levels in HepG2 cells enhanced 3.63–4.15 times (12.30 U/mg prot to 44.70–51.07 U/mg prot) than that of H_2O_2-treated group. The SOD assay exhibited that **14q** owned promising antioxidant profile of cellular SOD enzyme antioxidant system and was a potent antioxidant defense against cellular oxidative damage.

GSH is the most abundant non-protein thiol in eukaryotic cells, and a cofactor and co-substrate for a variety of antioxidant metabolic enzymes to repair damaged DNA and scavenges ROS [36]. The level of GSH can decrease following oxidative stress's formation and is a clear indicator of oxidative damage [42]. As showed in Fig. 7C, exposure of HepG2 cells to H_2O_2 for 12 h significantly reduced the GSH level from 81.33 to 39.87 μg/10^6 cell, whereas this effect was weaken by pretreating with compound **14q**. Specifically, the GSH level was 74.00, 64.47 and 42.00 μg/10^6 cell by **14q** at 50, 25 and 5 μM, respectively. This showed **14q** could display a positive effect of GSH non-enzymatic antioxidant system on reducing peroxidation, and provided an efficient protective role on oxidative injured cells induced by H_2O_2. The findings allow us to judge that **14q** could up-regulate the SOD and GSH content in oxidized cells, and

it was observed that exogenous antioxidants played a positive effect on fighting oxidative stress via enzymatic and non-enzymatic antioxidant system [29].

Hydroxytyrosol could easily be oxidized in either air or solution and be stabilized by esterification [13]. To verify whether compound **14q** improved its stability through the above way, the stability of **14q** and hydroxytyrosol were evaluated by evaluating their remaining percentage in methanol solution, which was placed at 25℃ or 50℃ for various times. As shown in Fig. 8, we found that the percentage of both **14q** and hydroxytyrosol were reduced with their exposure-time at the same temperature. Hydroxytyrosol decreased slowly at 25°C in four days, but decreased rapidly even in same days at 50°C. However, **14q** showed more stable than hydroxytyrosol at either 25℃ or 50℃. This indicated that conjugate **14q** was a more stable compound compared with hydroxytyrosol, and esterization strategy of hydroxytyrosol could improve its derivatives' stability.

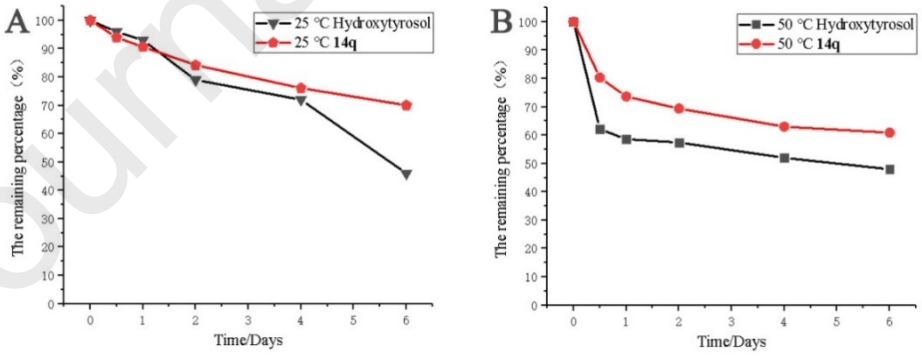

Fig. 8. The stability of hydroxytyrosol and **14q** in methanol at 25℃ (A) or 50℃ (B).

4. Conclusion

Based on the facts that excellent antioxidant activity of natural hydroxytyrosol and good bio-pharmacological activities of coumarin scaffold, we synthesized a series of conjugates of coumarin and hydroxytyrosol. The compounds were studied antioxidant activities, toxicity, and antioxidant mechanism of the compounds in vitro. The performed evaluation results showed that all conjugates displayed good free radicals scavenging activity, and several compounds with better free radicals scavenging activity also illustrated low toxicity properties compared to the standard controls. Especially, compound **14q** obtained satisfactory free radical scavenging activity and weak toxicity. In addition, **14q** effectively enhance the viability of H_2O_2-injured cells, and inhibit H_2O_2-induced oxidative apoptosis. Furthermore, **14q** enhanced intracellular key antioxidant enzyme SOD, regulated the glutathione redox system's status, and increased the content of non-enzymatic antioxidant GSH in H_2O_2-induced HepG2 cells. The findings allow us to judge that **14q** was a safe and effective synthetic antioxidant that protected cells from oxidative stress, and played a positive effect of enzymatic and non-enzymatic antioxidant system on fighting oxidative stress. Collectively, the results showed that **14q** is a potential antioxidant and deserves further investigation and development.

Acknowledge

This work was financially supported by the National Natural Sciences Foundations of China (No: 21672093).

Declaration of Competing Interest

The authors declare no conflict of interest.

Appendix A. Supplementary material

Supplementary data to this article can be found online at https://

References

[1] S. Chatterjee, Chapter Two-Oxidative Stress, Inflammation, and disease, Oxidative Stress and Biomaterials, 2016, 35–58.

[2] C. Nocella, V. Cammisotto, F. Pigozzi, P. Borrione, C. Fossati, A. D'Amico, R. Cangemi, M. Peruzzi, G. Gobbi, E. Ettorre, G. Frati, E. Cavarretta, R. Carnevale, S.M. Group, Impairment between oxidant and antioxidant systems: Short- and Long-term implications for Athletes' health, Nutrients 11 (2019) 1353.

[3] M.E. Zujko, A.M. Witkowska, A. Waśkiewicz, E. Sygnowska, Estimation of dietary intake and patterns of polyphenol consumption in Polish adult population, Adv. Med. Sci-poland. 57 (2012) 375–384.

[4] A. Augustyniak, G. Bartosz, A. Cipak, et al., Natural and synthetic antioxidants: an updated overview, Free Radic. Res. 44 (2010) 1216–1262.

[5] K. Haider, Md R. Haider, K. Neha, M.S. Yar, Free radical scavengers: An overview on heterocyclic advances and medicinal prospects. Eur. J. Med. Chem. 204 (2020) 112607.

[6] F. Visioli, D. Caruso, E. Plasmati, R. Patelli, N. Mulinacci, A. Romani, G. Galli, C. Galli, Hydroxytyrosol, as a component of olive mill waste water, is dose-dependently absorbed and increases the antioxidant capacity of rat plasma, Free Radic. Res. 34 (2001) 301–305.

[7] F. Visioli, C. Galli, E. Plasmati, S. Viappiani, A. Hernandez, C. Colombo, A. Sala, Olive phenol hydroxytyrosol prevents passive smoking–induced oxidative stress, Circulation 102 (2000) 2169–2171.

[8] I. Peluso, N.S. Yarla, R. Ambra, G. Pastore, G. Perry, MAPK signalling pathway in cancers: Olive products as cancer preventive and therapeutic agents, Semin. Cancer Biol. 56 (2019) 185–195.

[9] C. Vilaplana-Pérez, D. Auñón, L.A. García-Flores, A. Gil-Izquierdo, Hydroxytyrosol and potential uses in cardiovascular diseases, cancer, and AIDS, Front. Nutr. 1 (2014) 18.

[10] H. Wu, K. Jiang, T. Zhang, G. Zhao, G. Deng, Hydroxytyrosol exerts an anti-

inflammatory effect by suppressing Toll-like receptor 2 and TLR 2 downstream pathways in Staphylococcus aureus-induced mastitis in mice, J. Fun. Foods 35 (2017) 595–604.

[11] K. Yamada, H. Ogawa, A. Hara, Y. Yoshida, Y. Yonezawa, K. Karibe, V.B. Nghia, H. Yoshimura, Y. Yamamoto, M. Yamada, K. Nakamura, K. Imai, Mechanism of the antiviral effect of hydroxytyrosol on influenza virus appears to involve morphological change of the virus, Antivir. Res. 83 (2009) 35–44.

[12] M. Arunsundar, T.S. Shanmugarajan, V. Ravichandran, 3,4-Dihydroxyphenylethanol attenuates spatio-cognitive deficits in an Alzheimer's disease mouse model: Modulation of the molecular signals in neuronal survival-apoptotic programs, Neurotox. Res. 27 (2015) 143–155.

[13] A. Gambacorta, D. Tofani, R. Bernini, A. Migliorini, High-yielding preparation of a stable precursor of hydroxytyrosol by total synthesis and from the natural glycoside oleuropein, J. Agr. Food Chem. 55 (2007) 3386–3391.

[14] A. Procopio, C. Celia, M. Nardi, M. Oliverio, D. Paolino, G. Sindona, Lipophilic Hydroxytyrosol esters: Fatty acid conjugates for potential topical administration, J. Nat. Prod. 74 (2011) 2377–2381.

[15] S.S. Garga, J. Guptaa, S. Sharmab, D. Sahuc, An insight into the therapeutic applications of coumarin compounds and their mechanisms of action. E. J. Pharm. Sci. 152 (2020) 105424.

[16] K.V. Sairam, B.M. Gurupadayya, R.S. Chandan, K.N. Dattatri, B. Vishwanathan, A review on chemical profile of coumarins and their therapeutic role in the treatment of cancer, Curr. Drug Deliv. 13 (2016) 186–201.

[17] S. Sandhu, Y. Bansal, O. Silakari, G. Bansal, Coumarin hybrids as novel therapeutic agents, Bioorg. Med. Chem. 22 (2014) 3806–3814.

[18] S. Emami, S. Dadashpour, Current developments of coumarin-based anti-cancer agents in medicinal chemistry, Eur. J. Med. Chem. 102 (2015) 611–630.

[19] C.T. Dooley, R.A. Houghten, A comparison of combinatorial library approaches for the study of opioid compounds, Perspect. Drug Discov. 2 (1995) 287–304.

[20] S. Sana, V.G. Reddy, S. Bhandari, T.S. Reddy, R. Tokala, A.P. Sakla, S.K. Bhargava, N. Shankaraiah, Exploration of carbamide derived pyrimidine-thioindole conjugates as potential VEGFR-2 inhibitors with anti-angiogenesis effect, Eur. J. Med. Chem. 200 (2020) 112457.

[21] W.-T. Huang, J. Liu, J.-F. Liu, L. Hui, Y.-L. Ding, S.-W. Chen, Synthesis and biological evaluation of conjugates of deoxypodophyllotoxin and 5-FU as inducer of caspase-3 and -7, Eur. J. Med. Chem. 49 (2012) 48–54.

[22] Z.-B. Tang, Y.-Z. Chen, J. Zhao, X.-W. Guan, Y.-X. Bo, S.-W. Chen, L. Hui, Conjugates of podophyllotoxin and norcantharidin as dual inhibitors of topoisomerase Ⅱ and protein phosphatase 2A. Eur. J. Med. Chem. 123 (2016) 568–576.

[23] S.-Y. Hao, S.-L. Feng, X.-R. Wang, Z. Wang, S.-W. Chen, L. Hui, Novel conjugates of podophyllotoxin and coumarin: Synthesis, Cytotoxities, Cell cycle arrest and Inhibition of TOPO-Ⅱβ. Bioorg. Med. Chem. Lett. 29 (2019) 2129–2135.

[24] R. Rafique, K.M. Khan, Arshia, S. Chigurupati, A. Wadood, A.U. Rehman, U. Salar, V. Venugopal, S. Shamim, M. Taha, S. Perveen, Synthesis, in vitro α-amylase inhibitory, and radicals (DPPH & ABTS) scavenging potentials of new N-sulfonohydrazide substituted indazoles, Bioorg. Chem. 94 (2020) 103410.

[25] K.P. Cruz, M.M. Basualto, J.M. Valenzuela, G.B. Gonzalez, P.N. Encina, L.N. Vergara, J.A. Squella, C.O. Azar, Synthesis and antioxidant study of new polyphenolic hybrid-coumarins, Arab. J. Chem. 11 (2018) 525–537.

[26] G. Shevchenko, A. Anisimov, K. Suponitsky, Novel Mannich bases of α- and γ-mangostins: Synthesis and evaluation of antioxidant and membrane-protective activity. Eur. J. Med. Chem. 152 (2018) 10–20.

[27] Y. Yao, H. Wang, F. Xu, Y. Zhang, Z. Li, X. Ju, L. Wang, Insoluble-bound polyphenols of adlay seed ameliorate H_2O_2-induced oxidative stress in HepG2 cells via Nrf2 signalling, Food Chem. 325 (2020) 126865.

[28] Z. Chai, W. Huang, X. Zhao, H. Wu, X. Zeng, C. Li, Preparation, characterization,

antioxidant activity and protective effect against cellular oxidative stress of polysaccharide from Cynanchum auriculatum Royle ex Wight, Int. J. Bio. Macromol. 119 (2018) 1068–1076.

[29] Y.-O. Teng, X.-Z. Li, K. Yang, X.-H. Li, Z.-J. Zhang, L.-Y. Wang, Z.-J. Deng, B.-B. Song, Z.-H. Yan, Y.-Z. Zhang, K. Lu, P. Yu, Synthesis and antioxidant evaluation of desmethylxanthohumol analogs and their dimers, Eur. J. Med. Chem. 125 (2017) 335–345.

[30] J. Gliwa, A. Gunenc, N. Ames, W. G. Willmore, F. S. Hosseinian, Antioxidant activity of alkylresorcinols from Rye Bran and their protective effects on Cell Viability of PC-12 AC Cells, J. Med. Chem. 59 (21) (2011) 11473–11482.

[31] D.-J. Fu, J.-H. Li, J.-J. Yang, P. Li, Y.-B. Zhang, S. Liu, Z.-R. Li, S.-Y. Zhang, Discovery of novel chalcone-dithiocarbamates as ROS-mediated apoptosis inducers by inhibiting catalase, Bioorg. Chem. 86 (2019) 375–385.

[32] Y. Du, H.-F. Guo, H.-X. Lou, Grape seed polyphenols protect cardiac cells from apoptosis via induction of endogenous antioxidant enzymes, J. Agric. Food Chem. 55 (2007) 1695–1701.

[33] G.-Y. Liu, Y.-Z. Sun, N. Zhou, X.-M. Du, J. Yang, S.-J. Guo, 3,3′-OH curcumin causes apoptosis in HepG2 cells through ROS-mediated pathway, Eur. J. Med. Chem. 112 (2016) 157–163.

[34] A. Choudhary, A. Kumar, N. Kaur, ROS and oxidative burst: Roots in plant development, Plant Diversity 42 (2020) 33–43.

[35] H. Shirinzadeh, E. Neuhaus, E. Erguccd, A. T. Alyiev, H.-G. Orhanc, S. Suzenb, New indole-7-aldehyde derivatives as melatonin analogues; synthesis and screening their antioxidant and anticancer potential, Bioorg. Chem. 104 (2020) 104219.

[36] T. Kundu, B. Bhattacharjee, S. Hazra, A.K. Ghosh, D. Bandyopadhyay, A. Pramanik, Synthesis and biological assessment of pyrrolobenzoxazine scaffold as a potent antioxidant, J. Med. Chem. 62 (2019) 6315–6329.

[37] Y. An, J.-N. Li, Y.-J. Liu, M.-X. Fan,H. Shirinzadeh, E. Neuhaus, E. Erguccd, A.

T. Alyiev, H.-G. Orhanc, S. Suzenb, Neuroprotective effect of novel celecoxib derivatives against spinal cord injury via attenuation of COX-2, oxidative stress, apoptosis and inflammation, Bioorg. Chem. 101 (2020) 104044.

[38] V. Jurisic, S. Radenkovic, G. Konjevic, The actual role of LDH as tumor marker, biochemical and clinical aspects, Adv. Exp. Med. Biol. 867 (2015) 115–124.

[39] B.-C. Hu, Y. Liu, M.-Z. Zheng, R.-Y. Zhang, M.-X. Li, F.-Y. Bao, H. Li, L.-X. Chen, Triterpenoids from Anchusa italica and their protective effects on hypoxia/reoxygenation induced cardiomyocytes injury, Bioorg. Chem. 97 (2020) 103714.

[40] S.S. Raychaudhuri, X.W. Deng, The role of superoxide dismutase in combating oxidative stress in higher plants, Bot. Rev. 66 (2000) 89–98.

[41] F. Dashtestani, H. Ghourchian, A. Najafi, Albumin coated copper-cysteine nanozyme for reducing oxidative stress induced during sperm cryopreservation, Bioorg. Chem. 80 (2018) 621–630.

[42] H. Sies, Glutathione and its role in cellular functions, Free Radical Bio. Med. 27 (1999) 916–921.

Research highlights:

1. Twenty conjugates of coumarin and hydroxytyrosol were synthesized.
2. These conjugates showed potent antioxidant activities in DPPH and ABTS assays.
3. Compound **14q** exhibited less toxicity and weaker cytotoxicity.
4. Compound **14q** enhanced the cell viability of both H_2O_2-injured tumor HepG2 cells and normal WI-38 cells.
5. Compound **14q** induced production of ROS, inhibited the release of LDH and increased the production of SOD and GSH in H_2O_2-treated HepG2 cells.

Synthesis and antioxidant evaluation of conjugates of coumarin and hydroxytyrosol

Wen-Bo Li, Xue-Peng Qiao, Zi-Xiao Wang, Shuai Wang, Shi-Wu Chen *